

Portland State University

PDXScholar

Environmental Science and Management
Faculty Publications and Presentations

Environmental Science and Management

12-2020

Projected Impact of Mid-21st Century Climate Change on Wildfire Hazard in a Major Urban Watershed outside Portland, Oregon USA

Andy McEvoy

Portland State University

Max Nielsen-Pincus

Portland State University, maxnp@pdx.edu

Andres Holz

Portland State University, andres.holz@pdx.edu

Arielle J. Catalano

Portland State University, a.j.catalano@pdx.edu

Kelly E. Gleason

Portland State University, k.gleason@pdx.edu

Follow this and additional works at: https://pdxscholar.library.pdx.edu/esm_fac



Part of the [Forest Sciences Commons](#), and the [Sustainability Commons](#)

Let us know how access to this document benefits you.




Citation Details

McEvoy, A., Nielsen-Pincus, M., Holz, A., Catalano, A. J., & Gleason, K. E. (2020). Projected Impact of Mid-21st Century Climate Change on Wildfire Hazard in a Major Urban Watershed outside Portland, Oregon USA. *Fire*, 3(4), 70.

This Article is brought to you for free and open access. It has been accepted for inclusion in Environmental Science and Management Faculty Publications and Presentations by an authorized administrator of PDXScholar. Please contact us if we can make this document more accessible: pdxscholar@pdx.edu.

Article

Projected Impact of Mid-21st Century Climate Change on Wildfire Hazard in a Major Urban Watershed outside Portland, Oregon USA

Andy McEvoy ^{1,2,*} , Max Nielsen-Pincus ² , Andrés Holz ³ , Arielle J. Catalano ³ and Kelly E. Gleason ²

¹ USFS PNW Research Station ORISE Fellow, Corvallis, OR 97331, USA

² Department of Environmental Science and Management, Portland State University, Portland, OR 97201, USA; maxnp@pdx.edu (M.N.-P.); k.gleason@pdx.edu (K.E.G.)

³ Department of Geography, Portland State University, Portland, OR 97201, USA; andres.holz@pdx.edu (A.H.); acat2@pdx.edu (A.J.C.)

* Correspondence: andrew.mcevoy2@usda.gov

Received: 17 October 2020; Accepted: 3 December 2020; Published: 8 December 2020



Abstract: Characterizing wildfire regimes where wildfires are uncommon is challenged by a lack of empirical information. Moreover, climate change is projected to lead to increasingly frequent wildfires and additional annual area burned in forests historically characterized by long fire return intervals. Western Oregon and Washington, USA (westside) have experienced few large wildfires (fires greater than 100 hectares) the past century and are characterized to infrequent large fires with return intervals greater than 500 years. We evaluated impacts of climate change on wildfire hazard in a major urban watershed outside Portland, OR, USA. We simulated wildfire occurrence and fire regime characteristics under contemporary conditions (1992–2015) and four mid-century (2040–2069) scenarios using Representative Concentration Pathway (RCP) 8.5. Simulated mid-century fire seasons expanded in most scenarios, in some cases by nearly two months. In all scenarios, average fire size and frequency projections increased significantly. Fire regime characteristics under the hottest and driest mid-century scenarios illustrate novel disturbance regimes which could result in permanent changes to forest structure and composition and the provision of ecosystem services. Managers and planners can use the range of modeled outputs and simulation results to inform robust strategies for climate adaptation and risk mitigation.

Keywords: climate change; fire regime change; fire size; fsm; low frequency fire regime; western Oregon; wildfire risk

1. Introduction

Moist forests historically characterized by infrequent wildfire are projected to experience significant increases in wildfire frequency before the end of the century as a result of climate change and anthropogenic activities [1–3]. Many of these forests are not adapted to rapid shifts in disturbance regimes and future wildfire could lead to irreversible changes in vegetation structure and composition [4–7]. The pace and magnitude of climate change and resulting shifts in disturbance regimes could lead to reduced forest resilience, which, in this setting, refers to a reduced capacity of forests to continue to provide ecosystem services on which communities rely [6,8–11]. In the present, human communities rely on these forests for drinking water, economic value, carbon storage and sequestration, and cultural significance, but climate-wildfire adaptation strategies that would maintain resilience are underdeveloped [12–15].

In the United States, the region west of the Cascade Range crest in Oregon and Washington (westside) has historically been dominated by, but not limited to, infrequent, often stand-replacing fires [16]. Large fire occurrence on the westside is strongly linked to regional climate and weather patterns [17,18]. Westside forests are highly productive, as result of cool, wet maritime conditions, and although abundant, fuels are typically too wet to burn, let alone experience prolonged, severe weather that leads to large fires [17,19]. Unlike some other fire regimes, and because high and predictable winter rainfall rewets fuels, large westside wildfires are not strongly linked to long-term drought conditions (i.e., interannual), but rather appear to be closely tied to short-term drought immediately preceding and coinciding with the fire [20,21]. When an ignition does coincide with extremely dry fuel, fires can burn at extremely high intensity, usually defined as greater than 10,000 kW/m or flame lengths in excess of 4 m [22]. Likewise, ignitions coinciding with extremely dry fuel can lead to very large fires (>5000 ha) as a result of abundant, relatively continuous fuel [2,23]. Several events in mesic forests in westside forests in Oregon and Washington rank among the largest wildfire events in US history including the 1845 Great Fire (~600,000 ha) and the 1933 Tillamook Burn (~100,000 ha) both in the Oregon Coast Range and the 1865 Silverton Fire (~40,000 ha) and 1902 Yacolt Burn (~400,000 ha), both in the western Cascade Range of Oregon and Washington, respectively [24–27].

Climate change has raised average annual temperatures, increased the annual occurrence of short-term drought conditions, reduced snowpack and led to earlier peaks in summer streamflow in western Oregon and Washington [28–32]. Summer temperatures are projected to increase across the westside (e.g., +2 °C [33]), leading to lower average fuel moisture [34], doubling the historic area burned (e.g., 2010–2039 compared to 1961–2004 [35]; 2071–2100 compared to 1971–2000 [36]). In fact, average annual temperatures in western Oregon and Washington have already increased by nearly 1 °C over the 20th century [29,30]. There is less agreement on future annual precipitation patterns, but precipitation during the fire season is commonly projected to decrease [37–39]. Average snowpack in the West has dropped by up to 30% since 1915, and during the winter of 2014–2015, westside winter temperatures were 2–4 °C warmer than average, while snow water equivalent was reduced by as much as 30% [28,40]. Reduced snowpack and warmer winter temperatures have been leading to earlier peaks in summer streamflow, summer drought conditions and overall longer fire seasons in western Oregon [31,32,41].

Changes in westside fire regimes in the near future could have profound social impacts because westside communities are particularly dependent on surrounding forest ecosystems [42]. The overwhelming majority of Oregon and Washington's population lives on the westside and could be vulnerable to the direct threat of wildfires. Indirectly, westside communities are dependent on forests for a number of ecosystem services which could be impaired by projected fire regime shifts [10]. Westside communities largely rely on surface sources of drinking water [43]. The two largest westside population centers in the Pacific Northwest (PNW), Seattle, WA (metro population ~4 million, 51% of state) and Portland, OR (metro population ~2.5 million, 60% of state) both access the majority of their drinking water from mountain watersheds in the western Cascade Range. Surface drinking water source quality and quantity may suffer from a number of climate-wildfire related challenges such as post-fire debris slides, reduced downstream water yield where there is high demand from human communities, and changes in snow accumulation and snowmelt timing that reduce the volume and limit the availability of downstream supply [44–46]. Fire regime shifts could also lead to appreciably decreased productivity and as a result reduce the economic vitality of regional timber economies [47].

Characterizing contemporary and future wildfire risk exposure is complicated by varying definitions of fire regimes. Westside fire regimes are commonly characterized by infrequent, stand-replacing fires, largely explained by regional climate patterns [12,19]. However, patterns of fire frequency and severity are not monolithic across the westside and there is disagreement about how to best meaningfully classify westside fire regimes [16]. For instance, peer-reviewed studies increasingly point to a complex regional mosaic of fire size, frequency, and severity on the westside explained by local topography, micro-climates, and land management interacting with further spatially

variable and top-down regional climate controls [16,48–51]. The relatively limited empirical fire record and the overwhelming success of fire suppression efforts make it difficult to define and characterize contemporary westside fire regimes [52,53].

Given the regional heterogeneity in fire regime characteristics within the westside and limited direct experience with wildfire, managers and planners benefit from modeled assessments of fire regimes and fire risk to inform wildfire response, landuse planning, and climate adaptation [54–56]. To date, most assessments of future westside fire regime characteristics have relied on relatively coarse scale dynamic global vegetation models that fail to capture local variation in fire regime characteristics [41,57–59]. The LANDIS II model has also been used to forecast future changes in forest structure and composition, including as a result of wildfire [60]. However, Monte Carlo-based fire simulation models have become one of the most widely used techniques for conducting wildfire risk assessments at national, regional, and state levels [61,62]. Ref. [63] developed a novel technique for using the large fire simulator FSim, a Monte Carlo approach model, to project changes in future fire regimes over the Northern Rockies, but no similar studies have been conducted for the westside Cascade Range to the authors' knowledge.

The primary objective of this study was to characterize plausible mid–21st century changes in wildfire exposure to a municipal watershed in a way that captures locally specific spatial and temporal variation in fire regime characteristics. It is expected that such information will help managers and planners identify sources of risk and will inform development of risk mitigation and climate adaptation strategies. We selected the Clackamas River watershed (Clackamas Basin) east of Portland, Oregon because it is located in a region with spatially diverse fire regime characteristics and which has not experienced a very large fire (greater than ~5000 ha) in more than a century [16]. Additionally, the Clackamas Basin is the second largest source of drinking water for the Portland metro area. In 2017, the Eagle Creek Fire threatened Portland's primary drinking water source the Bull Run watershed adjacent to the Clackamas Basin, and elevated the importance of evaluating future fire exposure in municipal watersheds. Using a range of plausible climate scenarios for 2040–2069 and modeling methods presented in [63], we assessed the range of projected changes in fire size, frequency and seasonality of large fire events. In addition, we evaluated projected changes in the spatial distribution and magnitude of wildfire exposure to the watershed using a quantified hazard metric described in [64].

2. Materials and Methods

2.1. Study Area

Clackamas County, Oregon is part of the Portland metropolitan area and encompasses the majority of the Clackamas Basin. Portland is the largest metro area in Oregon with 2.5–3 million residents, only slightly smaller than the Seattle metro area. The Clackamas Basin, 244,002 ha, provides drinking water to over 300,000 Portland area residents and is the second largest drinking water source for the Portland region. Land ownership and management in the Clackamas Basin is heavily segmented (Figure 1). Approximately two-thirds of the watershed, the upper or higher elevation portion, is managed by the Mt. Hood National Forest (MHNF) (Table 1) division of the United States Forest Service (USFS). In the Clackamas Basin, the MHNF includes wilderness, motorized recreation areas, campsites and day-use facilities, and active timber management units. The middle portion of the watershed is comprised of a patchwork of land managed primarily for commercial timber value by the U.S. Bureau of Land Management (BLM) and a variety of private industrial timber landowners. The lower watershed transitions from very low-density rural development and agriculture to increasingly dense suburban and urban housing in the Portland metro area. Clackamas County's population is expected to grow by nearly 270,000 people in the next fifty years, placing increasing demand on land and water resources [65].

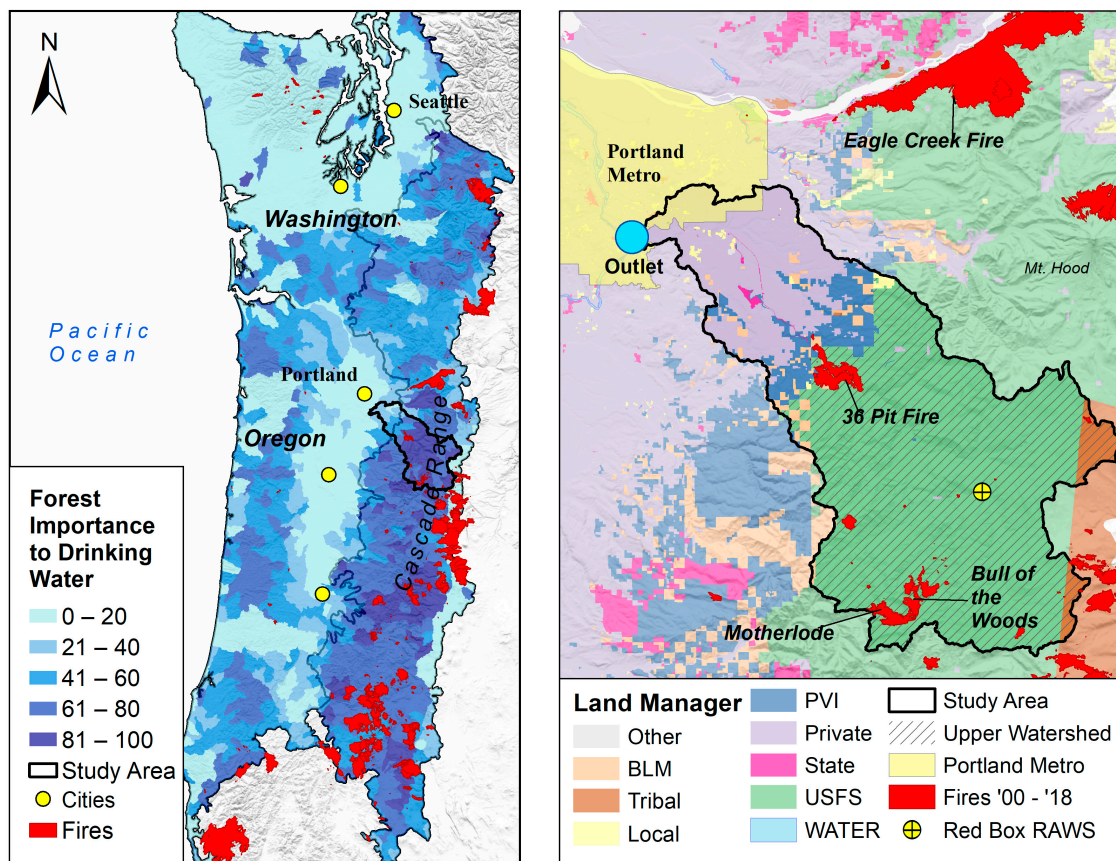


Figure 1. The westside region of Oregon and Washington shown on the left for context of the Clackamas Basin on the right. U.S. Forest Service “Forest to Faucets” [66,67] compares the importance of forests to surface drinking water on a relative scale of 0–100. Forests are especially important to drinking water in westside landscapes (left), many of which have experienced few to no significant wildfires in the past 20 years [27]. Prior to 2020, the largest wildfire in recent history in the Clackamas Basin (right) was the 36 Pit fire in 2014 which burned just over 2200 ha on the Mt. Hood National Forest, but adjacent to private land [68].

The basin ranges from the crest of the Cascade Range at approximately 2200 m in elevation, to about 3 m in elevation at the confluence of the Clackamas and Willamette Rivers (Figure 1). The Clackamas Basin is dominated by moist mixed-conifer forests largely characterized by western hemlock (*Tsuga heterophylla*) [69]. Potential vegetation types indicate that Clackamas Basin forest types are adapted to infrequent (>200 year fire return intervals) but stand replacing fires, as well as to moderately frequent fires (50–150 year return intervals) of mixed severity [16]. However, existing species assemblages and forest structure throughout much of the watershed are the result of human land management, predominantly the legacy of intensive forest management during the 20th century which favored relatively young, even-aged, and single species stands [70]. The vast majority of the watershed is coniferous forests (Table 1) including Douglas-fir (*Pseudotsuga menziesii* var. *menziesii*), western hemlock and Pacific silver fir (*Abies amabilis*) as well as other conifers in smaller extents. The watershed receives over 150–200 cm of precipitation on average annually, the vast majority of which falls between October and April each year [17,71]. The watershed has two main types of geology: the lower watershed is dominated by the older Western Cascade mountains (inactive with shallow subsurfaces), whereas the upper watershed (Figure 1) encompasses the younger High Cascades (with active Volcanoes) and porous geology [72]. Summers are generally dry, and, as a result of groundwater storage, seasonal variations in drought are highly dependent on snowpack levels and snowmelt

timing [32]. Although annual temperatures are moderate, late summer temperatures regularly exceed 32 °C during same period of time when water resources are most scarce.

Table 1. Major land manager groups in the Clackamas Basin and associated land cover. Rows may not sum to 100% because of miniscule amounts of other landcover, including non-burnable landcover (i.e., rock, ice and certain types of row crops), water, grasslands and exotic plants. USFS = U.S. Forest Service; Private = private, non-industrial; PVI = private, industrial timber; Federal = other federal entities including U.S. Fish and Wildlife, Bureau of Indian Affairs; BLM = U.S. Bureau of Land Management; Local = county and municipal; State = state of Oregon.

Manager	Total Area (ha)	Percent of Study Area	Non-Vegetated	Developed	Agricultural	Hardwood	Conifer
USFS	167,663	69%	1%	0%	0%	0%	98%
Private	47,358	19%	1%	14%	36%	12%	34%
PVI	14,130	6%	1%	1%	1%	7%	85%
Federal	6878	3%	0%	0%	5%	0%	88%
BLM	5697	2%	0%	0%	0%	7%	90%
Local	1490	1%	2%	8%	20%	5%	59%
State	691	0%	6%	12%	12%	16%	51%

Ref. [16] characterize the Clackamas Basin as a ‘moderate-frequency/mixed-severity’ fire regime. The national LANDFIRE dataset indicates that fire return intervals greater than 200 years dominate the mid- and low-elevation portions of the watershed, approximately 55% of the watershed, while the upper watershed, where lightning strikes are more common and forests are drier, return intervals are between 35 and 200 years [73]. Despite thousands of recorded ignitions in the Clackamas Basin from 1992–2015, nearly 75% of which are caused by human-activities there have been only a handful of large fire events in recent history (Figure 1) [74]. The fact that most ignitions do not result in a large fire reflects mostly the lack of fire conducive climate/weather conditions as well as the fact that most human ignitions are identified immediately and able to be quickly extinguished (i.e., campfires, equipment fires, and escaped brush piles). At the time of this writing, one of the largest wildfires on record is actively burning in the watershed. Favored by very dry and hot, fast-moving easterly winds that rapidly cured fuels, within days the Riverside Fire ignited on 7 September 2020 and was just one of several major fires during one of the largest wildfire events in western Oregon’s recorded history. Within days the Riverside Fire grew to nearly 60,000 hectares; the cause is listed as unknown but is not suspected to be lightning. Prior to the Riverside Fire, the 36 Pit Fire burned just over 2000 hectares in the middle of the watershed in 2014, and the B & B Complex fires in the southeast of the watershed in 2003 covered over 30,000 hectares, some of which were located in the uppermost section of the watershed.

2.2. Wildfire Modeling

We used the large fire simulator, FSim, to model contemporary fire regime characteristics and wildfire exposure as well as the effect of climate change during 2040–2069 (mid-century) [75]. FSim uses a Monte Carlo approach to model the interaction of fuel, topography, weather and spatial ignition patterns on a daily time-step and simulate fire occurrence, growth and suppression in thousands of statistically plausible, unique fire seasons. For calibration and modeling purposes, large fires were defined as fires greater than or equal to 100 hectares. The particulars of FSim as well as probabilistic fire risk assessments have been well documented elsewhere [62,63,75–78]. We simulated contemporary and future wildfire occurrence in two model domains in order to reasonably account for all fires that might ignite outside but spread into the Clackamas Basin, similar to recent experience with, for example, the B & B Complex fires (Figure 2). The upper reaches of the Clackamas Basin about the Cascade Range crest which divides two drastically different fire environments, but records show that fires can and do ignite on the east side of the mountains and spread west into the watershed (e.g., as what the Lionshead fire did on 7 September 2020). For each domain, east and west, we used unique fire histories,

model inputs, and climate data described below, simulated 10,000 fire seasons for each model domain, and combined and clipped the outputs to the Clackamas Basin.

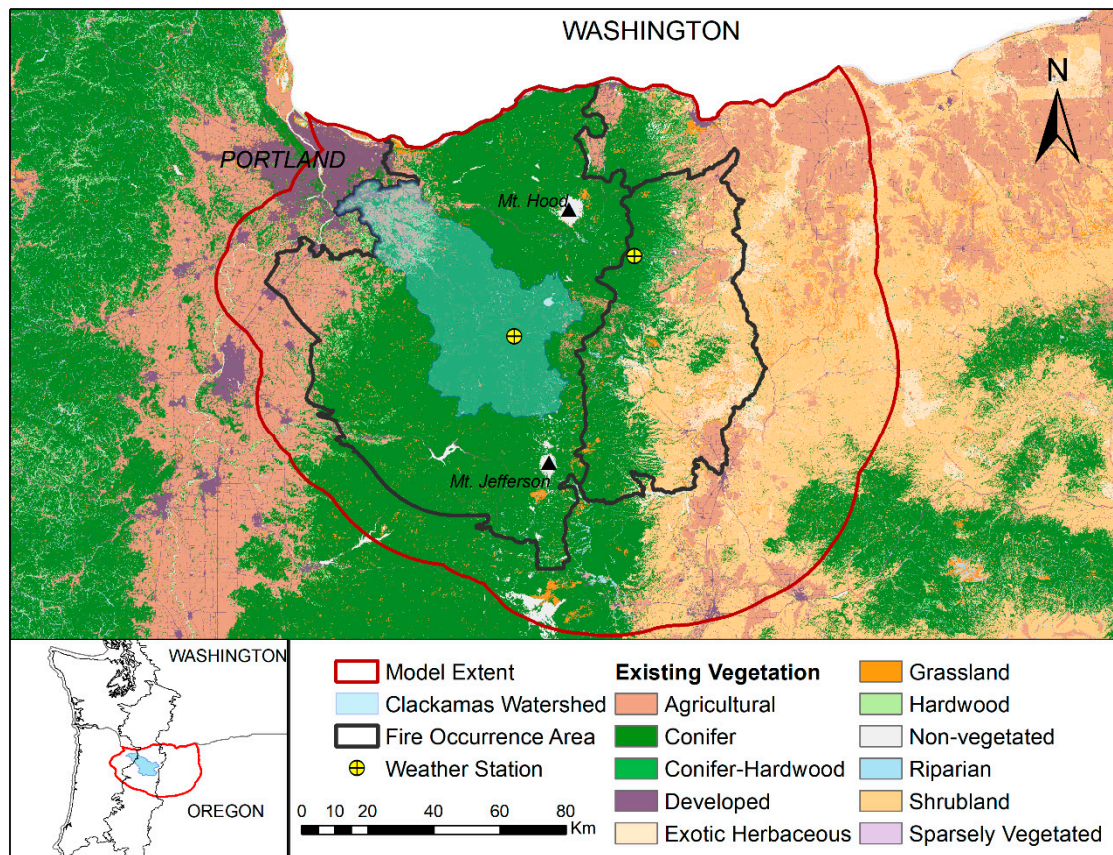


Figure 2. Extent of FSim modeling. The model extent was divided into two fire occurrence areas (FOAs) in order to distinguish between very different fire environments on either side of the Cascade Range crest. Each FOA was associated with a unique weather station from which empirical observations were used in the baseline scenarios, and modified to reflect projected future climate conditions. The FOA defines the area within which FSim simulated ignitions and is significantly larger than the analysis area, the Clackamas Basin, in order to allow for fires that ignite outside the analysis area but eventually burn into it.

We used daily weather records (1992–2015) from two Remote Automated Weather Stations (RAWS) (Figure 2). RAWS data were processed in Fire Family Plus software to compute a distribution of daily Energy Release Component values based on Fuel Model G (ERC-G) [75,79]. ERC quantifies the amount of energy released at the flaming front of an active fire and is a proxy for fuel moisture and ERC-G was selected because [80] demonstrated its utility across a range vegetation types, including closed canopy conifer forests which dominate the Clackamas Basin as well as dry forests, and shrublands in the eastern FOA (Figure 2) [63,75,81]. FSim uses ERC to determine on what days a fire may ignite, how many fires may ignite, and when fires do ignite FSim uses ERC values in conjunction with wind speed/direction and landscape features to simulate how a fire grows and is extinguished.

To simulate mid-century climate scenarios we adapted methods from [63]. We selected four global climate models (GCMs) from the Coupled Model Intercomparison Project phase 5 (CMIP 5). CMIP5 GCMs have been evaluated for use and applied across the PNW, including the study area [59,82]. Each model was downscaled from native to 4 km resolution using the Multivariate Adaptive Constructed Analogs (MACA) method which was specifically designed for wildfire applications [83]. Only Representative Concentration Pathway (RCP) 8.5 scenarios were considered based on guidance from local resource managers who expressed a primary concern for

high emissions scenarios. Models were selected based on average annual changes in temperature and relative humidity over the Clackamas Basin between historical (1970–1999) and mid-century periods. Among the nineteen available GCMs CNRM-CM5 (CNRM), HadGEM-ES365 (HadGEM), MIROC5, and MIROC-ESM-CHEM (MIROCHEM) represent the outer boundaries of possible changes in mid-century temperature and relative humidity. All four GCMs project warmer average annual temperatures in mid-century, but MIROCHEM and MIROC5 project increased average annual relative humidity where CNRM and HadGEM project a decrease in relative humidity. HadGEM is the warmest and driest GCM, CNRM is dry and slightly less warm than HadGEM, MIROCHEM is warm and more humid, while MIROC 5 is the coolest and wettest GCM. Projected monthly average changes in temperature and relative humidity were used to augment observed RAWs data and create a distribution of ERC values that reflect plausible mid-century ERC values (Figure 3).

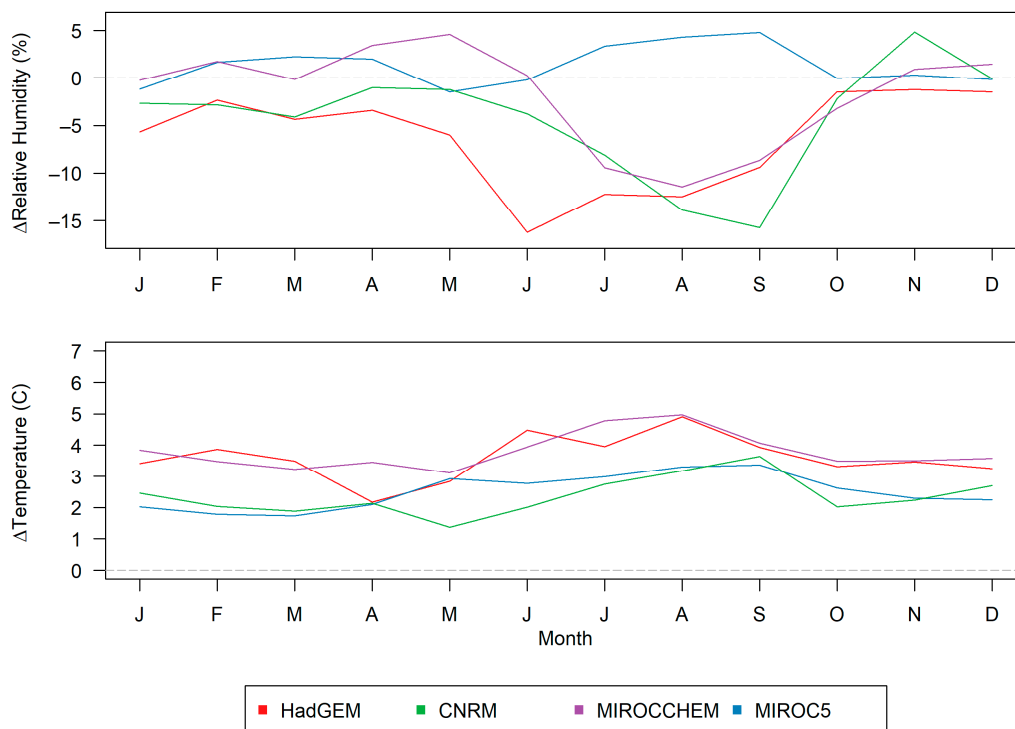


Figure 3. Average monthly temperature and relative humidity departure from historical (1970–1999) predicted by the four GCMs selected to model future fire weather conditions. These four GCMs represent a full range of predicted climate futures and were downscaled over the study area.

We generated an ignition probability raster quantifying the relative likelihood of an ignition at any pixel in the Clackamas Basin using historical ignitions of fires greater than 100 hectares in the Fire Program Analysis, Fire Occurrence Dataset [74]. A raster stack of eight 90 m resolution LANDFIRE layers were used as inputs for each model domain to describe topography and fuels [84–91]. The same landscape files were used in baseline and mid-century scenarios.

2.3. Data Analysis

For each scenario, we merged simulated fire perimeters from the two domains (east and west of the Cascade Range crest) and removed the overburn. Overburn occurred when fires from the same simulation year burned the same pixel(s); the fire perimeter which ignited earlier in the year was maintained and overburnt pixels were removed from the subsequent fire. Under baseline conditions and in the least warm mid-century scenarios overburn was less than 5%, but in the hot and dry mid-century scenarios it was as high as 12%. After correcting for overburn, we generated new burn probability rasters for the Clackamas Basin that reflected the occurrence of fires from both domains

east and west of the Cascade Range crest. All spatial and quantitative analysis was performed in R statistical software 3.5 [92].

Fire season timing and length were measured using average daily ERC values. Our treatment of ERC and fire season is similar to that in [63], which used the relationship between ERC and National Fire Danger Rating System classifications to measure fire season. The bottom threshold for “moderate fire danger” and an indication of active fire season, was defined by the 80th percentile ERC values [93]. The 80th percentile was derived from baseline climate data and was applied to all mid-century scenarios because the fuel moisture thresholds to fire occurrence are not expected to change. We also calculated the number of days on which daily average ERC values exceeded the 90th (“high fire danger”) and 97th (“extreme fire danger”) percentiles for all scenarios.

Using the overburn-corrected perimeters we calculated average annual number of fires, average fire size, and average annual area burned to evaluate the impact of changes in temperature and relative humidity associated with potential future climate change effects. Fire size and annual area burned distributions from all four mid-century scenarios were compared to baseline using a Mann-Whitney test with an alpha of 0.05. Fire size distributions were compared between the four mid-century scenarios using a Kruskal-Wallis test followed by Dunn’s Multiple Pairwise Comparison using the Benjamini-Hochberg adjustment method with an alpha of 0.05. In addition to annual metrics, we included two unique fire characteristic analyses. First, we sub-sampled 300 thirty-year samples of fire perimeters for each climate scenario to evaluate the variation in annual area burned during each thirty-year climate period. FSim uses a Monte Carlo simulation approach in which each iteration is assigned a year and represents a statistically plausible annual fire season and, because the weather module is dynamic and ignitions are stochastic, each iteration is unique. [94] presented a method for subsampling the 10,000 iterations to create statistically plausible multidecadal scenarios. Similar to [94], each iteration was assigned a “fire year” and within each thirty-year sample, we assumed that the same pixel would not burn more than once every five years and removed overlapping portions of fire perimeters when they were within five years of each other. A multidecadal analysis is particularly useful in low frequency fire regimes in contrast to metrics like annual averages which may reveal trends over time, but have little managerial application.

Second, modeling studies elsewhere have demonstrated the value in assessing trends over time in the frequency and magnitude of extremely large fires [95,96]. In this study, extremely large fires are fires that exceed 99th percentile fire size under baseline climate conditions (9861 ha). In addition to evaluating climate change impacts on average fire size, we used a generalized Pareto distribution model to evaluate trends in the size and return intervals of extremely large (99th percentile) fires. Generalized Pareto models have been used to evaluate probabilities in the tails of highly skewed distributions in which, like wildfire, extremely rare events are highly impactful [97]. Extreme event analysis was performed in R using the ‘extRemes’ package [92,98].

Finally, [64] introduced a metric that quantifies integrated wildfire hazard as the product of burn probability and mean fireline intensity at each pixel in the study area. This method has the advantage of being quantitative and easily comparable across space and time, aiding managers to identify areas that are at highest risk of burning at high intensity. Evaluating the potential intensity of future fires is particularly important where risk to drinking water is concerned [99–101]. We calculated integrated hazard for all burnable pixels for each climate scenario and determined the change in hazard that results from all four GCMs. All spatial analyses are presented using quantiles of the modeled data distribution.

3. Results

3.1. Fire Season

Three of four future scenarios project that the fire season as measured by ERC will expand by mid-century (Figure 4). Under baseline conditions 80th percentile ERC value was 29, 90th percentile

was 39 and 97th percentile was 51. There were on average 70 days above 80th percentile ERC in the baseline scenario. In Figure 4, MIROC5, the least warm and wettest of the GCMs, shows an eight day increase in average fire season length but it is not significantly different than baseline (Mann-Whitney, $p = 0.289$). The remaining three GCMs project significantly higher ERC values between May and November. MIROCCHM and CNRM both projected 99 days above the 80th percentile (Mann-Whitney, $p < 0.0001$), and HadGEM projected 102 days on average each year during which ERC values will be above the 80th percentile (Mann-Whitney, $p < 0.0001$). Under HadGEM climate conditions ERC values exceeded the 80th percentile earlier in the season but peaked in August and September similar to baseline conditions. In contrast MIROCCHM and CNRM models illustrated the potential for a similar start to fire season compared to today, but the peak might not occur until late September or October. Seasonal changes in ERC from Figure 4 were reflected in the seasonal pattern and magnitude of simulated ignitions where HadGEM simulated large numbers of fires in July and August, while MIROCCHM and CNRM simulated more fires late in the summer and early fall (Figure 5).

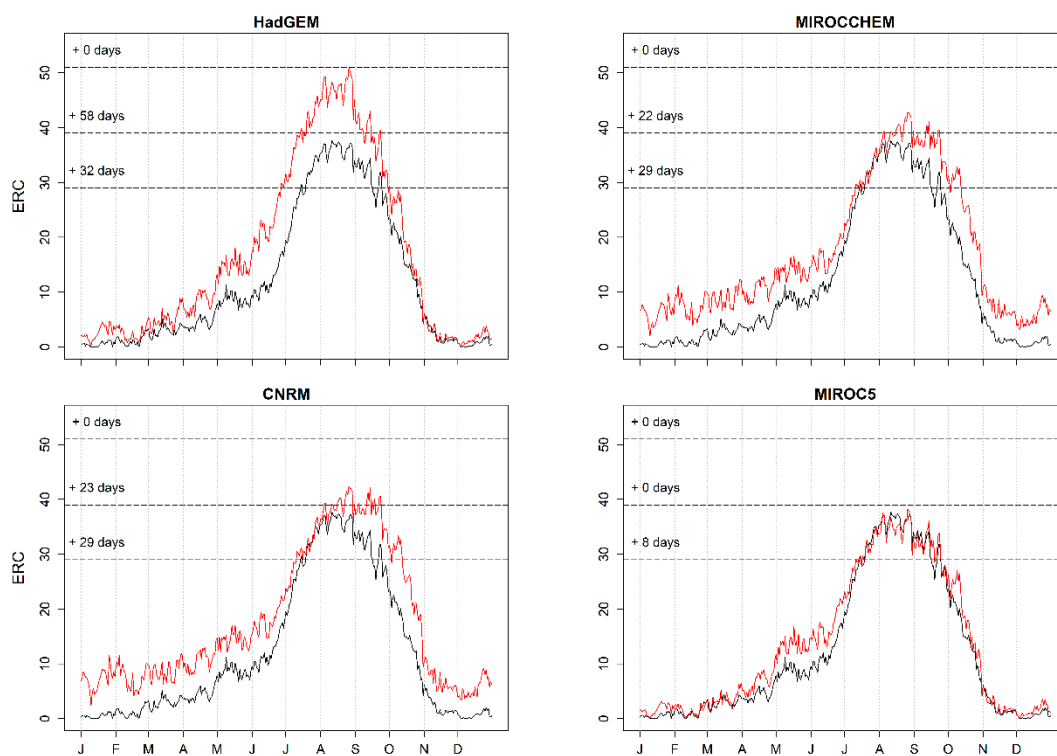


Figure 4. Mean daily ERC values for each future (2040–2069) climate scenario, shown in red, compared to baseline ERC values, shown in black. Dashed horizontal lines reflect the 80th, 90th, 97th, ERC percentiles based on the 1992–2015 baseline climate. Numbers above the dashed lines indicate the number of days additional to baseline during which fire weather exceeds each fire danger rating.

Under baseline conditions, average daily ERC values never exceeded 90th percentile ERC, the high fire danger threshold. Daily ERC values are highly variable from one year to the next and have exceeded 90th percentile thresholds, but average daily baseline ERC values do not. In contrast, HadGEM, CNRM, and MIROCCHM projected more severe fire weather with 33–69 days on average exceeding 90th percentile ERC (Mann-Whitney, $p < 0.0001$) (Figure 4). No scenarios projected average daily ERC values above the 97th percentile extreme fire danger threshold, but HadGEM projected average ERC will be close to the 97th percentile throughout August and September.

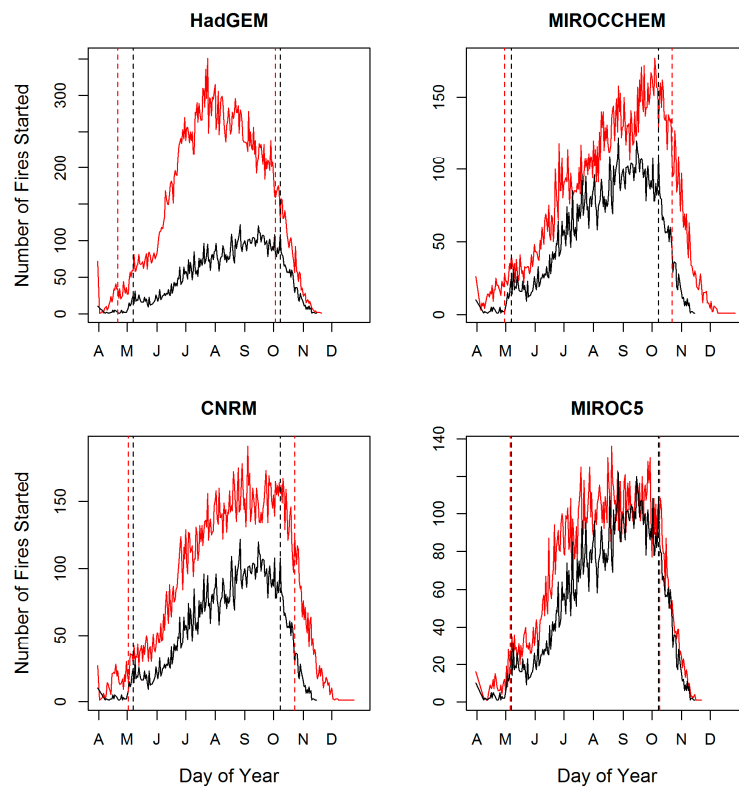


Figure 5. Number of simulated fires as a function of day of year for mid-century scenarios (red) and baseline (black). Vertical dotted lines indicate period during which fires greater than 100 ha account for more than 90% of the annual area burned on average.

3.2. Large Fire Size and Frequency

In response to longer fire seasons and longer continuous stretches of fire-conductive weather within each season, the average annual number and size of simulated large fires increased under each of the climate scenarios compared to baseline (Table 2). Increased large fire occurrence in mid-century simulations mirrors seasonal ERC patterns (Figure 4). Under all mid-century climate conditions there were more projected opportunities for ignitions to occur, and higher potential for ignitions to turn into large fires. The size and probability of extremely large wildfire events also increased under mid-century conditions. The largest fire simulated under baseline conditions was 37,509 ha. The largest fire size increased significantly (Mann-Whitney, $p < 0.001$) to 42,899 ha under MIROC5, 45,051 ha under MIROCCHM, 68,152 ha under HadGEM, and 71,646 ha under CNRM.

Accordingly, changes in fire size and frequency generally resulted in increased annual area burned. Excluding fire-free years, approximately 1200 ha burned annually on average under baseline conditions (Table 2). Compared to baseline, projected annual average area burned increased significantly ($p < 0.001$) by 50% under MIROC5, 95% under MIROCCHM, nearly 150% under CNRM, and 540% under HadGEM. Projected annual area burned was significantly different among all scenarios, not just between mid-century and baseline scenarios (Dunn's test, $p < 0.01$). Under baseline conditions during years in which fires occurred, less than 0.5% of the watershed burned, but the average extent of the watershed burned on average increased to 1% under CNRM and over 3% under HadGEM. However, the range of projected annual area burned values in Table 2 illustrates that large regions of the watershed could be impacted in a given year under any of the scenarios, including baseline, in which the largest annual area burned was 56,656 ha, or 23% of the watershed.

Table 2. Simulated mean fire size of all fires and the mean annual number of large fires, fires greater than 100 ha. Range and standard error are shown below mean values. Conditional area burned is the size of the study area effected in those years that fires were simulated—not all years experienced fire. 30-year area burned is the estimated cumulative extent of wildfire between 2040–2069. Mid-century fire size and frequency distributions were compared to baseline distributions using Dunn’s tests and in all instances, mid-century distributions were significantly different from baseline (all $p < 0.0001$).

Scenario	Annual Average			30 Year Average	
	Mean Fire Size (ha)	Number of Large Fires	Area Burned (ha)	Number of Large Fires	Area Burned (ha)
Baseline	587	0.36	1177	10.85	18,745
range	<1–37,509	0–9	<1–56,656	2–31	194–95,110
SE	±19.01	±0.009	±35.7	±0.4252	854
MIROC5	794	0.54	1837	16.07	32,194
range	<1–42,899	0–7	<1–61,730	2–37	3439–133,842
SE	±21.16	±0.010	±50.2	±0.303	1125
MIROCHEM	864	0.73	2295	22.00	43,278
range	<1–45,051	0–11	<1–86,162	7–53	6201–184,097
SE	±20.21	±0.012	±62.5	±0.382	1451
CNRM	999	0.89	2828	26.63	55,514
range	<1–71,646	0–11	<1–90,732	10–55	4674–142,224
SE	±20.85	±0.012	±67.2	±0.429	1498
HadGEM	1759	1.88	7542	56.32	137,616
range	<1–68,152	0–12	<1–102,730	0–140	31,745–262,257
SE	±23.57	±0.015	±125	±1.400	2275

When we sub-sampled the 10,000 iterations in each scenario and created thirty-year samples we learned that increasingly more of the watershed will be exposed to wildfire during the mid-century. Under baseline conditions approximately 8% of the watershed is projected to experience wildfire in a thirty-year period. From 2040–2069, a projected 13% of the watershed would be affected under the MIROC5 scenario, 18% under MIROCHEM, 23% under CNRM, and 56% of watershed under HadGEM.

Extremely large wildfires are fires exceeding the 99th percentile of modeled fire sizes in each scenario. Compared to baseline conditions, the number and size of extremely large fires is projected to increase under all mid-century climate scenarios (Table 3). Under baseline conditions the average extremely large fire was 15,789 ha (sd = 5808). This average increased significantly under MIROC5 (mean = 19,917 ha, sd = 6193), under MIROCHEM (mean = 22,104 ha, sd = 6628), under CNRM (mean = 23,254 ha, sd = 7392), and under HadGEM (mean = 30,746 ha, sd = 7334). A generalized Pareto model illustrated that the threshold for extremely large fires is projected to increase by more than a factor of two (Table 3). Likewise, fires with a 0.01 probability of occurrence are projected to be increasingly larger (Table 3).

Table 3. Results from a generalized Pareto distribution (GPD) model of 99th percentile fire sizes under each climate scenario. The threshold of fire sizes for consideration was set at the 99th percentile of each scenario’s fire size distribution. Shape parameters close to 0 indicate that fire size distributions are light-tailed exponential and negative values indicate that fire sizes are finite. 100- and 1000-Year return intervals (RI) refer to the fire size (ha) with a 0.01 and 0.001 probability of occurrence.

Peak over Threshold Results	Baseline	MIROC5	MIROCHEM	CNRM	HadGEM
Threshold (ha), μ	9861	13,199	14,597	16,011	22,651
Number of fires	114	148	195	219	350
Shape, ξ	0.00	−0.09	−0.01	0.03	−0.01
100 Year RI (ha)	10,537	15,974	19,789	21,526	33,452
1000 Year RI (ha)	25,853	30,493	34,469	38,460	49,645

Annualized metrics are useful for illustrating the effect of climate change on fire characteristics, but results demonstrate that fire occurrence will continue to vary intra- and inter-annually. In all future scenarios there were iterations during the 10,000 simulations during which no fires were simulated because ERC never exceeded 80th percentile values, or because simulated ignitions occurred but were located in unburnable pixels (i.e., water or urbanized areas). We can interpret iterations without fire as “fire free years”. Under baseline conditions, 43% of iterations included no fires. However, climate change is projected to decrease the number of fire free years in mid-century. 36% of iterations were fire free under MIROC5, 27% under MIROCCHM, 23% under CNRM, and 18% under HadGEM.

3.3. Wildfire Hazard

Wildfire hazard under baseline conditions is concentrated at higher elevations in the upper watershed where both burn probability and mean fireline intensity are highest (Figure 6). Increases in wildfire hazard under all mid-century climate scenarios were driven by increased burn probability (Figure 7). Increased fire size and more frequent wildfires resulted in 226%, 357%, and 476% of average watershed-wide increases, compared to baseline, in burn probability in MIROC5, MIROCCHM, and CNRM, respectively. However, under the hot and dry conditions of HadGEM, average burn probability increased by 1663% (Table 4). Despite large changes in burn probability the actual annual likelihood of wildfire remains less than 1% across the entire watershed in all mid-century scenarios, except for HadGEM under which the watershed-wide average probability of wildfire in any given year exceeds 2% (Table 4). The distribution of mid-century burn probabilities across the watershed is similar to the spatial pattern in baseline conditions but under hotter and drier conditions, the lower and upper watershed became increasingly fire prone (Figure 8).

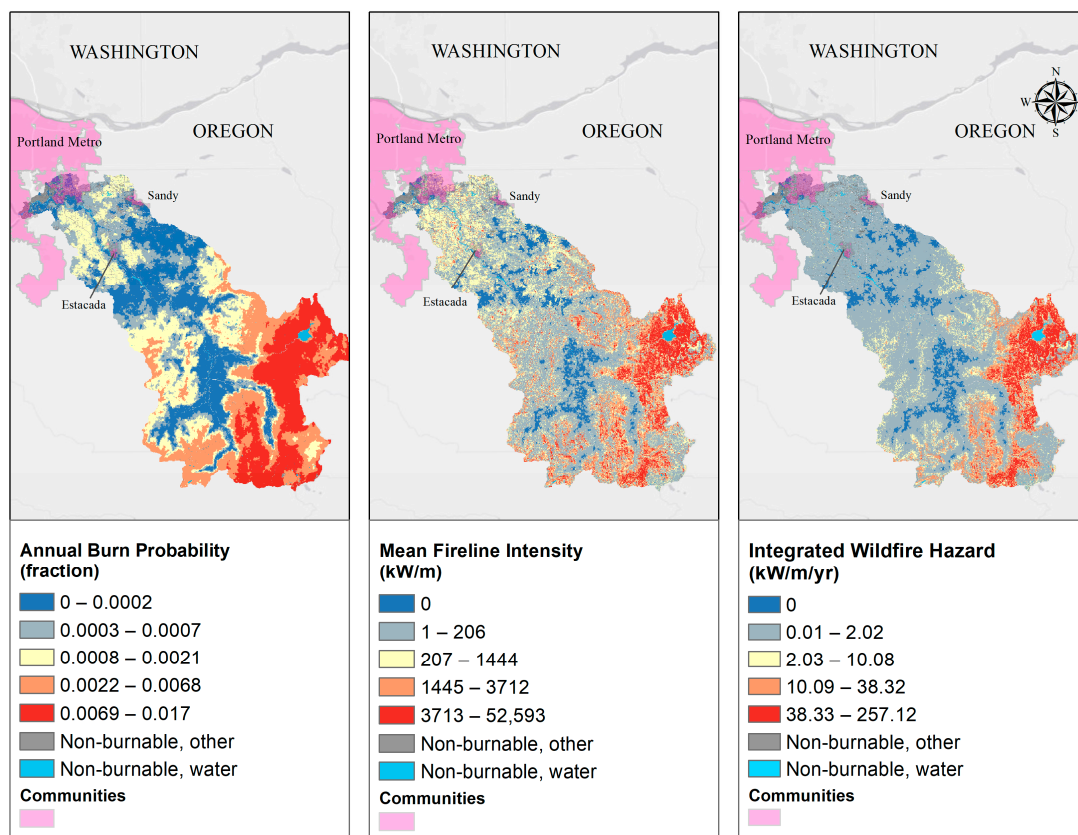


Figure 6. Wildfire behavior metrics under baseline conditions (1992–2015). Wildfire simulations produced maps of average annual burn probability (left) and mean fireline intensity (center) which, when multiplied, measure average wildfire hazard (right). Non-burnable pixels include water, barren land, development, and some types of agriculture.

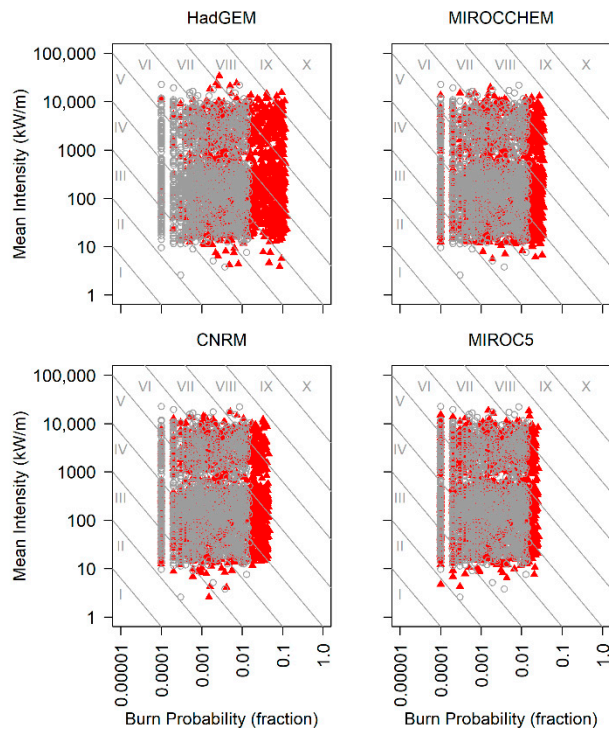


Figure 7. Burn probability and mean fireline intensity at each pixel in the study area under baseline (gray) and future scenarios (red). Diagonal lines demarcate integrated wildfire hazard classes.

Table 4. Watershed-wide average integrated wildfire hazard and hazard components under each climate scenario. Range and standard error are shown below each average value.

Scenario	Burn Probability (years ⁻¹)	Mean Intensity (kW/m)	Integrated Hazard (kW/m-year)
Baseline	0.003	1140	8.01
range	0.0001–0.017	0.749–52,593	7.49×10^{-5} –257
SE	$\pm 6.88 \times 10^{-6}$	± 4.38	± 0.041
MIROC5	0.005	1109	13.43
range	0.0001–0.028	0.415–41,066	4.15×10^{-5} –472
SE	$\pm 1.17 \times 10^{-5}$	± 4.08	± 0.068
MIROC5CHEM	0.007	1116	20.87
range	0.0001–0.038	0.818–97,725	9.95×10^{-5} –583
SE	$\pm 1.71 \times 10^{-5}$	± 3.99	± 0.095
CNRM	0.009	1125	24.29
range	0.0001–0.057	0.551–31,419	5.51×10^{-5} –968
SE	$\pm 2.22 \times 10^{-5}$	± 4.08	± 0.126
HadGEM	0.025	1158	71.57
range	0.0001–0.140	0.830–93,566	1.57×10^{-4} –2895
SE	$\pm 6.06 \times 10^{-5}$	± 4.34	± 0.358

Mean fireline intensity did not change as a result of changes in temperature and relative humidity (Table 3 and Figure 7). Mean fireline intensity in the watershed varies by approximately one order of magnitude from the lower watershed where the average value is about 300 kW/m to the upper watershed where the average value is about 3000 kW/m. Compared to baseline, none of the mid-century mean fireline intensities were significantly different (Mann-Whitney, $p > 0.05$).

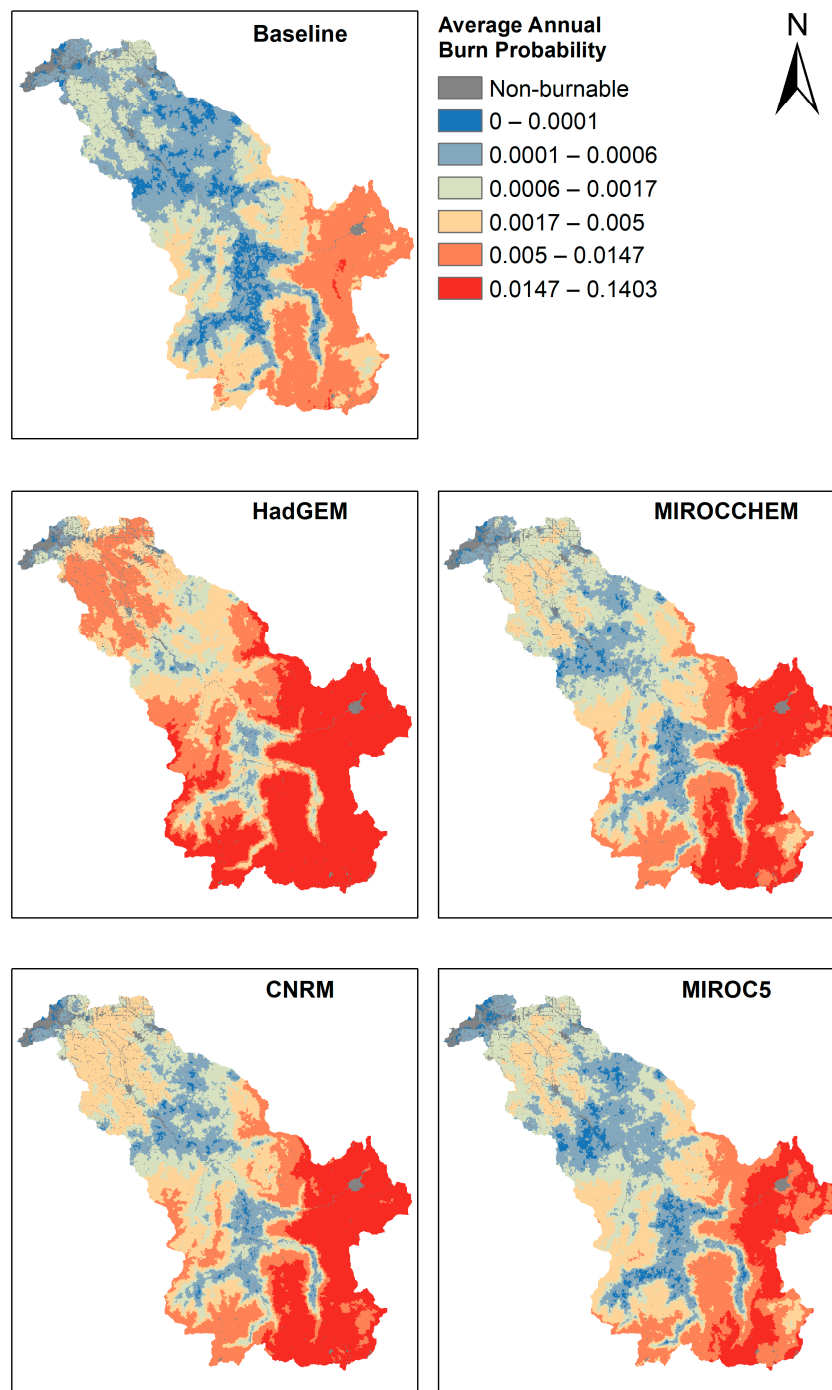


Figure 8. Average annual burn probability in the Clackamas Basin under baseline (1992–2015) and four mid-century (2040–2069) scenarios. HadGEM is the warmest and driest future scenario, followed by CNRM. Both MIROC5 and MIROC5 project small increases in summer relative humidity and are less hot than HadGEM and CNRM but are still warmer than baseline conditions. Non-burnable pixels indicate water, rock/ice, high density urban areas, and agriculture. Results are classified using a quantile method.

Increases in future wildfire hazard roughly follow the same spatial pattern as under baseline conditions with increasing hazard under hotter and drier conditions (Figure 9). In baseline conditions, approximately 30,000 ha (12%) are classified as very high hazard (Figure 9), but under mid-century conditions, very high hazard classifications increased to 37,000 ha (15%), 42,000 ha (17%), 45,000 ha (18%), and 62,000 ha (26%) under MIROC5, MIROC5, CNRM, and HadGEM, respectively. Under

CNRM and HadGEM, the lower watershed adjacent to the Portland metro area is exposed to increasing wildfire hazard (Figure 9).

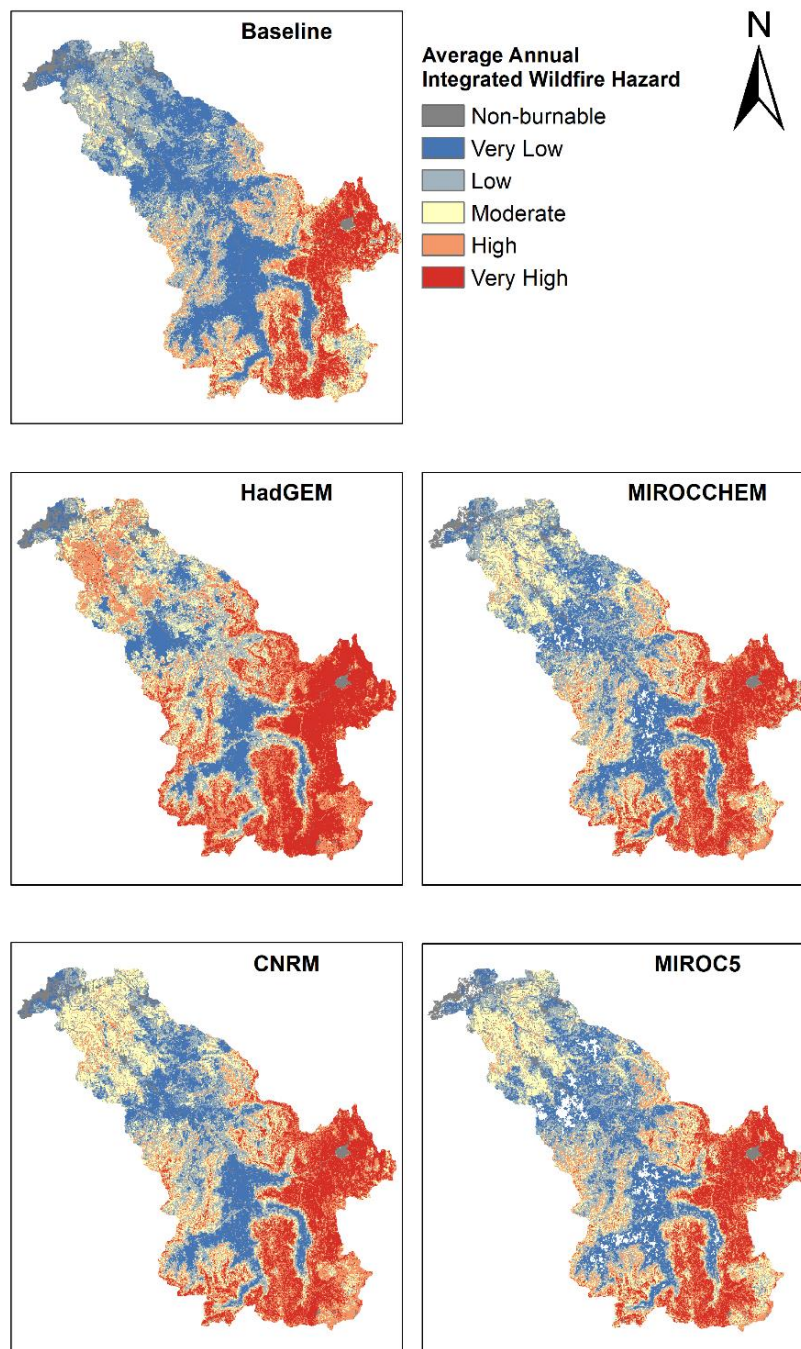


Figure 9. Integrated wildfire hazard is the product of annual burn probability and mean fireline intensity. Baseline wildfire hazard (upper left) under climate conditions based on empirical climate data 1992–2015. The four mid-century scenarios are based on projected climate scenarios. HadGEM is the warmest and driest future scenario, followed by CNRM. Both MIROCCHM and MIROC5 project small increases in summer relative humidity and are less hot than HadGEM and CNRM, but are still warmer than baseline conditions. Non-burnable pixels indicate water, rock/ice, high density urban areas, and agriculture. Results are classified using a quantile method.

4. Discussion

The primary objective of this study has been to characterize plausible impacts of climate change on mid-century wildfire hazard in a major municipal watershed which has experienced few recent large fires, but which has a demonstrated potential for infrequent, stand-replacing fires. Our results show that while wildfire hazard in the Clackamas Basin could significantly increase in the near future, the magnitude of change is uncertain because of variability in projections of future climate.

Our analysis projects an average three week increase in fire season length between baseline and mid-century time periods. Our methods were based on [63] which projected only a 12 day increase in average fire season length in the Northern Rocky Mountains of the United States. There are many factors which could explain the difference including very different biophysical settings, but also the fact that [63] used climate data representing a moderate emissions scenario. We used RCP 8.5, a scenario in which little to no action is taken to curb global emissions and which has been shown to be consistent with actual emissions [102]. However, contrasting research shows that RCP 8.5 may be less accurate for mid-century projections compared to more moderate emissions pathways and so our results should be interpreted as being based on plausible, but high end climate change projections [103]. [59] demonstrated that RCP 4.5 scenarios produce more moderate impacts on fire regime characteristics across the PNW, including the westside, compared to RCP 8.5. Likewise, our projections of longer future fire seasons could be moderated based on changes in future precipitation amount and seasonal timing. For instance, in a study that included western Oregon and Washington, [59] noted that earlier autumn precipitation could offset changes in temperature which might otherwise lead to longer fire seasons, but there is a high degree of uncertainty around future precipitation patterns [34,39,82].

Based on our method, future wildfire hazard in the Clackamas Basin will be largely a function of changes in annual burn probability, which we project could increase between 66–730%. Our assessment used simulation methods very similar to the PNW Quantitative Wildfire Risk Assessment (QWRA) but baseline burn probability values from our study were sometimes higher than burn probability modeled in the QWRA [104]. In particular, in the upper Clackamas Basin we projected burn probabilities as much as 80% greater than the QWRA (0.007109 compared to 0.003931). In part, the difference could be explained by our inclusion of simulated fires that ignited east of the Cascade Range, outside the Clackamas Basin, and spread into the basin. For regional and national fire simulations conducted with FSim, like the QWRA, it is not standard practice to account for fires transmitted between fire occurrence areas because of associated computational demands [94]. However, the top of the Clackamas Basin along the crest of the Cascade Range is a relatively low saddle and forests east of the crest are prone to significantly more frequent fires which have in the past spilled over onto the westside (i.e., B & B Fire in 2003). Our inclusion of fires transmitted across the saddle from east to west demonstrates the value of conducting simulations at a relatively local scale. In our analysis, generally longer fire seasons and more severe fire weather facilitated increases in burn probability which are consistent with recent studies of future westside fire frequency and annual area burned. Estimates of mid- and late-21st century annual area burned in westside study areas range from increases of 76–500% and our results indicate a similar range of the 56–540% increase in the Clackamas Basin [41,58]. Under hotter and drier conditions, we project that mid-century annual burn probabilities (in excess of 1.5%) in the upper Clackamas Basin will be increasingly similar to contemporary burn probabilities in high-frequency fire regimes like those of central Oregon, which arguably represents a new disturbance regime that would plausibly lead, through flammability feedbacks, to changes in dominant forest types [4,11,104–106].

Notably, our results showed no significant difference in future fireline intensity compared to baseline. Fireline intensity is a function of fuel type, fuel load, fuel moisture and rate of spread [107,108]. In FSim, fuel type and load are determined by fire behavior fuel models (FBFM) which were not changed between baseline and mid-century simulations, and the third, rate of spread, is strongly influenced by fuel structure, slope, and wind speed which also were not changed between baseline and mid-century simulations. The decision to not alter future FBFM and vegetation characteristics was based on research showing relatively stable westside forest structure and composition into

mid-century [58,59]. Despite the fact that fireline intensity appears to be best explained by fuel structure and wind speed, we did anticipate that modeled changes in temperature and relative humidity would result in lower fuel moisture in the future which would in turn facilitate higher mean fireline intensity in the Clackamas Basin [109,110]. In one study of projected future fireline intensity across Canada, [110] showed a 20% increase in the occurrence of fireline intensities high enough to limit ground and aerial suppression under RCP 8.5 in the near future. However, future fireline intensities in [110] were spatially heterogeneous and strongly associated with particular FBFM, so we might not expect similar results in the Clackamas Basin. In contrast, [111], similar to this study, found little to no change in mid-century conditional flame lengths, a fire intensity metric derived from fireline intensity. Fireline intensity is an important metric for understanding fire effects on vegetation, soil, and ecological processes, and it also informs wildfire response strategies [112,113]. Yet, wildfire simulations have been shown to underestimate fire intensity during severe fire weather events and so future work should focus on evaluating the sensitivity of modeled fireline intensity to fuel structure, wind speed and fuel moisture in westside forest types, as well as evaluating the accuracy of simulated fireline intensity under severe weather [114].

In addition to increased wildfire hazard in the future, extremely large wildfires are increasingly plausible in the Clackamas Basin. In fact, at the time of this writing, current events are demonstrating the plausibility of extreme westside wildfires. On 7 September 2020 a strong east wind, low relative humidity, and record temperatures fueled western Oregon wildfires to burn in excess of 300,000 hectares. One of those fires, the Riverside Fire (~56,000 ha and 72% contained) has burned nearly 40,000 hectares in the Clackamas Basin, very similar to the largest single-fire area burned that we simulated under baseline climate conditions (37,509 ha). The Riverside Fire confirms that westside landscapes are vulnerable to infrequent, large fires and that simulated very large fire sizes are not unrealistic. Our results indicate that very large fire sizes could increase significantly and that very large fires could be as much as eight times more frequent. This is consistent with [115] which projected an approximate fivefold increase in fires greater than 20,000 ha across the PNW under RCP 8.5. in mid-century. In a study of future fire size across Canada, [116] found that increasingly severe fire weather led to more days conducive to fire growth and a three to nine fold increase in the occurrence of extremely large wildfires. However, both [115] and [116] illustrate that projections of future fire sizes are closely linked to the emissions scenario, in which case our results ought be interpreted as plausible, but high-end projections of future fire sizes in the Clackamas Basin.

Our results demonstrate the importance of and provide an opportunity for climate adaptation and risk reduction planning in westside forests. The objective of this paper was to provide information that will be locally actionable for planners and managers in the Clackamas Basin, but we stop short of attempting to evaluate potential adaptation strategies. Our results illustrate a wide range of plausible future wildfire hazard, and, given that uncertainty, robust adaptation plans will be ones that maintain essential ecosystem services across the broadest range of future hazard scenarios [8,117,118]. Ref. [12] recommends continued, strategic fire suppression as a way to maintain ecosystem services in westside forests characterized by infrequent, stand replacing fires. However, our results project that fires could be burning more frequently under severe weather conditions which would limit the success of suppression and lead to higher costs [119,120]. Moreover, suppression in and of itself is not an effective land management strategy and could proliferate negative feedbacks and inhibit post-wildfire drought-adapted vegetation transitions [112,113]. A logical next step is for managers to assess likely consequences to specific resources and assets (i.e., timber value, water quality, communities, etc.) and then to use methods like those presented in [54,121–123], to develop climate adaptation strategies that balance forest management, fire suppression, and community preparedness to achieve a range of risk reduction goals.

5. Conclusions

This study simulated a plausible range of changes to mid-century fire regimes in a historically low- to moderate-frequency fire regime in western Oregon, USA. Simulation models in relatively low-frequency fire regimes are useful risk planning tools given the lack of actual wildfires in recent history, and the concentration of resources and assets. Moreover, projecting future fire regime characteristics is important given that climate change is projected to create annual conditions more conducive to large fires.

Our results demonstrated that wildfire hazard will likely increase by mid-century as a result of larger, more frequent fires. Future wildfires are expected to grow larger as fire weather conducive to large fires becomes more common and longer lasting. Projected changes in temperature and relative humidity led to longer fire seasons and more severe fire weather in three of the four scenarios. Under the hottest and driest mid-century scenarios, annual burn probabilities were similar to those found in higher frequency fire regimes. All climate and baseline scenarios illustrate that extremely large, intense fires are plausible, and that they will become more plausible under hotter and drier climate scenarios. The range of plausible impacts to mid-century fire regimes should be cause for managers and planners to adopt robust approaches to climate adaptation and risk mitigation. The hottest and driest mid-century scenarios could lead to disturbance regime changes resulting in significant changes to forest structure and composition, and as a result could pose significant challenges to ecosystem service provision. Even under more moderate mid-century climate scenarios, infrequent and very large wildfires remain a potential threat to ecosystems and communities.

Our work provides actionable information for regional managers and planners to guide decisions around climate adaptation in land use management, wildfire management, forest management, water provision and other fields which would be affected by wildfire. Ongoing research aims to evaluate the relative importance of fuel structure, fuel moisture and wind speed on fire size and intensity in westside forests. Based on this study, future work is needed to develop and test risk mitigation strategies that might be effective given the uncertainty demonstrated in mid-century fire regime characteristics. Finally, our results do not specifically address the role of rare wind events, such as those that led to the catastrophic westside fires in 2020. Additional work evaluating the ability of FSim to capture these events would be beneficial and supplement our analysis.

Author Contributions: Conceptualization, A.M., M.N.-P., A.H.; methodology, A.M., M.N.-P., A.H., K.E.G., A.J.C.; modeling, A.M., A.J.C.; analysis, A.M., A.J.C.; writing—original draft preparation, A.M.; writing—review and editing, A.M., M.N.-P., A.H., K.E.G.; visualization, A.M.; supervision, A.M., M.N.-P.; project administration, A.M., M.N.-P.; funding acquisition, M.N.-P., A.H. All authors have read and agreed to the published version of the manuscript.

Funding: A.M. was supported in part by an appointment to the United States Forest Service (USFS) Research Participation Program administered by the Oak Ridge Institute for Science and Education (ORISE) through an interagency agreement between the U.S. Department of Energy (DOE) and the U.S. Department of Agriculture (USDA). c All opinions expressed in this paper are the author's and do not necessarily reflect the policies and views of USDA, DOE, or ORAU/ORISE. AH was partially supported by National Science Foundation award # 1738104.

Acknowledgments: We would like to acknowledge support and guidance from Kim Swan and the Clackamas River Water Provider as well as Matt Glazewski and Clackamas County Water and Environment Services. Thank you to Paul Loikith for guidance in GCM selection. Thank you also to Portland State's Institute of Sustainable Solutions and the rest of the Clackamas team. Cody Evers, Alex Dye and Karin Riley provided input and technical support for FSim.

Conflicts of Interest: The authors declare no conflict of interest.

References

1. Buma, B.; Batllori, E.; Bisbing, S.; Holz, A.; Saunders, S.C.; Bidlack, A.L.; Creutzburg, M.K.; DellaSala, D.A.; Gregovich, D.; Hennon, P.; et al. Emergent freeze and fire disturbance dynamics in temperate rainforests. *Austral Ecol.* **2019**, *44*, 812–826. [[CrossRef](#)]

2. Krawchuk, M.A.; Moritz, M.A.; Parisien, M.A.; Van Dorn, J.; Hayhoe, K. Global Pyrogeography: The Current and Future Distribution of Wildfire. *PLoS ONE* **2009**, *4*, e5102. [[CrossRef](#)] [[PubMed](#)]
3. Mariani, M.; Holz, A.; Veblen, T.T.; Williamson, G.; Fletcher, M.-S.; Bowman, D.M.J.S. Climate Change Amplifications of Climate-Fire Teleconnections in the Southern Hemisphere. *Geophys. Res. Lett.* **2018**, *45*, 5071–5081. [[CrossRef](#)]
4. Kitzberger, T.; Aráoz, E.; Gowda, J.H.; Mermoz, M.; Morales, J.M. Decreases in Fire Spread Probability with Forest Age Promotes Alternative Community States, Reduced Resilience to Climate Variability and Large Fire Regime Shifts. *Ecosystems* **2012**, *15*, 97–112. [[CrossRef](#)]
5. McDowell, N.G.; Allen, C.D.; Anderson-Teixeira, K.; Aukema, B.H.; Bond-Lamberty, B.; Chini, L.; Clark, J.S.; Dietze, M.; Grossiord, C.; Hanbury-Brown, A.; et al. Pervasive shifts in forest dynamics in a changing world. *Science* **2020**, *368*, eaaz9463. [[CrossRef](#)]
6. McWethy, D.B.; Higuera, P.E.; Whitlock, C.; Veblen, T.T.; Bowman, D.M.; Cary, G.J.; Haberle, S.G.; Keane, R.E.; Maxwell, B.D.; McGlone, M.S.; et al. A conceptual framework for predicting temperate ecosystem sensitivity to human impacts on fire regimes: Evaluating human impacts on fire regimes. *Glob. Ecol. Biogeogr.* **2013**, *22*, 900–912. [[CrossRef](#)]
7. Sommerfeld, A.; Senf, C.; Buma, B.; D’Amato, A.W.; Després, T.; Díaz-Hormazábal, I.; Fraver, S.; Frelich, L.E.; Gutiérrez, Á.G.; Hart, S.J.; et al. Patterns and drivers of recent disturbances across the temperate forest biome. *Nat. Commun.* **2018**, *9*, 4355. [[CrossRef](#)]
8. Folke, C.; Carpenter, S.; Walker, B.; Scheffer, M.; Elmqvist, T.; Gunderson, L.; Holling, C.S. Regime Shifts, Resilience, and Biodiversity in Ecosystem Management. *Annu. Rev. Ecol. Evol. Syst.* **2004**, *35*, 557–581. [[CrossRef](#)]
9. Folke, C.; Carpenter, S.; Walker, B.; Scheffer, M.; Chapin, T.; Rockstrom, J. Resilience Thinking: Integrating Resilience, Adaptability and Transformability. *Ecol. Soc.* **2010**, *15*, 20. [[CrossRef](#)]
10. Seidl, R.; Spies, T.A.; Peterson, D.L.; Stephens, S.L.; Hicke, J.A. Review: Searching for resilience: Addressing the impacts of changing disturbance regimes on forest ecosystem services. *J. Appl. Ecol.* **2016**, *53*, 120–129. [[CrossRef](#)]
11. Whitlock, C.; McWethy, D.B.; Tepley, A.J.; Veblen, T.T.; Holz, A.; McGlone, M.S.; Perry, G.L.; Wilmshurst, J.M.; Wood, S.W. Past and Present Vulnerability of Closed-Canopy Temperate Forests to Altered Fire Regimes: A Comparison of the Pacific Northwest, New Zealand, and Patagonia. *BioScience* **2015**, *65*, 151–163. [[CrossRef](#)]
12. Halofsky, J.S.; Donato, D.C.; Franklin, J.F.; Halofsky, J.E.; Peterson, D.L.; Harvey, B.J. The nature of the beast: Examining climate adaptation options in forests with stand-replacing fire regimes. *Ecosphere* **2018**, *9*, e02140. [[CrossRef](#)]
13. McWethy, D.B.; Schoennagel, T.; Higuera, P.E.; Krawchuk, M.; Harvey, B.J.; Metcalf, E.C.; Schultz, C.; Miller, C.; Metcalf, A.L.; Buma, B.; et al. Rethinking resilience to wildfire. *Nat. Sustain.* **2019**, *2*, 797–804. [[CrossRef](#)]
14. Stephens, S.L.; Agee, J.K.; Fule, P.Z.; North, M.P.; Romme, W.H.; Swetnam, T.W.; Turner, M.G. Managing Forests and Fire in Changing Climates. *Science* **2013**, *342*, 41–42. [[CrossRef](#)]
15. Turner, M.G.; Donato, D.C.; Romme, W.H. Consequences of spatial heterogeneity for ecosystem services in changing forest landscapes: Priorities for future research. *Landsc. Ecol.* **2013**, *28*, 1081–1097. [[CrossRef](#)]
16. Spies, T.A.; Stine, P.A.; Gravenmier, R.; Long, J.W.; Reilly, M.J. *Synthesis of Science to Inform Land Management within the Northwest Forest Plan Area*; U.S. Department of Agriculture, Forest Service, Pacific Northwest Research Station: Portland, OR, USA, 2018.
17. Gedalof, Z.; Peterson, D.L.; Mantua, N.J. Atmospheric, Climatic, and Ecological Controls on Extreme Wildfire Years in the Northwestern United States. *Ecol. Appl.* **2005**, *15*, 154–174. [[CrossRef](#)]
18. Meyn, A.; White, P.S.; Buhk, C.; Jentsch, A. Environmental drivers of large, infrequent wildfires: The emerging conceptual model. *Prog. Phys. Geogr. Earth Environ.* **2007**, *31*, 287–312. [[CrossRef](#)]
19. Agee, J.K. *Fire Ecology of Pacific Northwest Forests*; Island Press: Washington, DC, USA, 1993.
20. Batllori, E.; De Cáceres, M.; Brotons, L.; Ackerly, D.D.; Moritz, M.A.; Lloret, F. Cumulative effects of fire and drought in Mediterranean ecosystems. *Ecosphere* **2017**, *8*, e01906. [[CrossRef](#)]
21. Stavros, E.N.; Abatzoglou, J.; Larkin, N.K.; McKenzie, D.; Steel, E.A. Climate and very large wildland fires in the contiguous western USA. *Int. J. Wildland Fire* **2014**, *23*, 899–914. [[CrossRef](#)]

22. Scott, J.H.; Thompson, M.P.; Calkin, D.E. *A Wildfire Risk Assessment Framework for Land and Resource Management*; U.S. Department of Agriculture, Forest Service, Rocky Mountain Research Station: Ft. Collins, CO, USA, 2013.
23. Bessie, W.C.; Johnson, E.A. The Relative Importance of Fuels and Weather on Fire Behavior in Subalpine Forests. *Ecology* **1995**, *76*, 747–762. [[CrossRef](#)]
24. Holbrook, S. *Burning an Empire: The Story of American Forest Fires*; The Macmillan Co.: New York, NY, USA, 1943.
25. Kemp, J.L. *Epitaph for the Giants: The Story of the Tillamook Burn*; Touchstone Press: Portland, OR, USA, 1967.
26. Morris, W.G. Forest Fires in Western Oregon and Western Washington. *Or. Hist. Q.* **1934**, *35*, 313–339.
27. National Interagency Fire Center. Historically Significant Wildfires 2020. Available online: https://www.nifc.gov/fireInfo/fireInfo_stats_histSigFires.html (accessed on 1 July 2020).
28. Cooper, M.G.; Nolin, A.W.; Safeeq, M. Testing the recent snow drought as an analog for climate warming sensitivity of Cascades snowpacks. *Environ. Re. Lett.* **2016**, *11*, 084009. [[CrossRef](#)]
29. Abatzoglou, J.T.; Barbero, R. Observed and projected changes in absolute temperature records across the contiguous United States. *Geophys. Res. Lett.* **2014**, *41*, 6501–6508. [[CrossRef](#)]
30. Mote, P.W.; Parson, E.A.; Hamlet, A.F.; Keeton, W.S.; Lettenmaier, D.; Mantua, N.; Miles, E.L.; Peterson, D.W.; Peterson, D.L.; Slaughter, R.; et al. Preparing for Climatic Change: The water, salmon, and forests of the Pacific Northwest. *Clim. Chang.* **2003**, *61*, 45–88. [[CrossRef](#)]
31. Jung, I.-W.; Chang, H. Assessment of future runoff trends under multiple climate change scenarios in the Willamette River Basin, Oregon, USA. *Hydrol. Process.* **2011**, *25*, 258–277. [[CrossRef](#)]
32. Tague, C.; Grant, G.E. Groundwater dynamics mediate low-flow response to global warming in snow-dominated alpine regions: Groundwater Dynamics and Low-Flow Response. *Water Resour. Res.* **2009**, *45*. [[CrossRef](#)]
33. McKenzie, D.; Gedalof, Z.; Peterson, D.L.; Mote, P. Climatic Change, Wildfire, and Conservation. *Conserv. Biol.* **2004**, *18*, 890–902. [[CrossRef](#)]
34. Mote, P.W.; Salathé, E.P. Future climate in the Pacific Northwest. *Clim. Chang.* **2010**, *102*, 29–50. [[CrossRef](#)]
35. Kitzberger, T.; Falk, D.A.; Westerling, A.L.; Swetnam, T.W. Direct and indirect climate controls predict heterogeneous early-mid 21st century wildfire burned area across western and boreal North America. *PLoS ONE* **2017**, *12*, e0188486. [[CrossRef](#)]
36. Davis, R.; Yang, Z.; Yost, A.; Belongie, C.; Cohen, W. The normal fire environment—Modeling environmental suitability for large forest wildfires using past, present, and future climate normals. *For. Ecol. Manag.* **2017**, *390*, 173–186. [[CrossRef](#)]
37. Dalton, M.M.; Shell, K.M. Comparison of Short-Term and Long-Term Radiative Feedbacks and Variability in Twentieth-Century Global Climate Model Simulations. *J. Clim.* **2013**, *26*, 10051–10070. [[CrossRef](#)]
38. Holden, Z.A.; Swanson, A.; Luce, C.H.; Jolly, W.M.; Maneta, M.; Oyler, J.W.; Warren, D.A.; Parsons, R.; Affleck, D. Decreasing fire season precipitation increased recent western US forest wildfire activity. *Proc. Natl. Acad. Sci. USA* **2018**, *115*, E8349–E8357. [[CrossRef](#)] [[PubMed](#)]
39. Schoof, J.T. High-resolution projections of 21st century daily precipitation for the contiguous U.S. *J. Geophys. Res. Atmos.* **2015**, *120*, 3029–3042. [[CrossRef](#)]
40. Mote, P.W.; Li, S.; Lettenmaier, D.P.; Xiao, M.; Engel, R. Dramatic declines in snowpack in the western US. *Npj. Clim. Atmos. Sci.* **2018**, *1*, 1–6. [[CrossRef](#)]
41. Rogers, B.M.; Neilson, R.P.; Drapek, R.; Lenihan, J.M.; Wells, J.R.; Bachelet, D.; Law, B.E. Impacts of climate change on fire regimes and carbon stocks of the U.S. Pacific Northwest. *J. Geophys. Res.* **2011**, *116*, G03037. [[CrossRef](#)]
42. Peterson, D.L.; Halofsky, J.E.; Johnson, M.C. Managing and adapting to changing fire regimes in a warmer climate. In *The Landscape Ecology of Fire*; Springer: Dordrecht, The Netherlands, 2011; pp. 249–267.
43. Brown, T.C.; Hobbins, M.T.; Ramirex, J.A. Spatial Distribution of Water Supply in the Coterminous United States. *J. Am. Water Resour. Assoc.* **2008**, *44*, 1474–1487. [[CrossRef](#)]
44. Wondzell, S.M.; King, J.G. Postfire erosional processes in the Pacific Northwest and Rocky Mountain regions. *For. Ecol. Manag.* **2003**, *178*, 75–87. [[CrossRef](#)]
45. Nolin, A.W. Perspectives on Climate Change, Mountain Hydrology, and Water Resources in the Oregon Cascades, USA. *Mt. Res. Dev.* **2012**, *32*, S35–S46. [[CrossRef](#)]

46. Gleason, K.E.; Nolin, A.W. Charred forests accelerate snow albedo decay: Parameterizing the post-fire radiative forcing on snow for three years following fire: Charred Forests Accelerate Snow Albedo Decay. *Hydrol. Process.* **2016**, *30*, 3855–3870. [[CrossRef](#)]
47. Latta, G.; Temesgen, H.; Adams, D.; Barrett, T. Analysis of potential impacts of climate change on forests of the United States Pacific Northwest. *For. Ecol. Manag.* **2010**, *259*, 720–729. [[CrossRef](#)]
48. Bakker, J.D.; Jones, E.; Sprenger, C.B. Evidence of a historical frequent, low-severity fire regime in western Washington, USA. *Can. J. For. Res.* **2019**, *49*, 575–585. [[CrossRef](#)]
49. Hessburg, P.F.; Spies, T.A.; Perry, D.A.; Skinner, C.N.; Taylor, A.H.; Brown, P.M.; Stephens, S.L.; Larson, A.J.; Churchill, D.J.; Povak, N.A.; et al. Tamm Review: Management of mixed-severity fire regime forests in Oregon, Washington, and Northern California. *For. Ecol. Manag.* **2016**, *366*, 221–250. [[CrossRef](#)]
50. Reilly, M.J.; Dunn, C.J.; Meigs, G.W.; Spies, T.A.; Kennedy, R.E.; Bailey, J.D.; Briggs, K. Contemporary patterns of fire extent and severity in forests of the Pacific Northwest, USA (1985–2010). *Ecosphere* **2017**, *8*, e01695. [[CrossRef](#)]
51. Tepley, A.J.; Swanson, F.J.; Spies, T.A. Fire-mediated pathways of stand development in Douglas-fir/western hemlock forests of the Pacific Northwest, USA. *Ecology* **2013**, *94*, 1729–1743. [[CrossRef](#)] [[PubMed](#)]
52. Bowman, D.M.; Balch, J.; Artaxo, P.; Bond, W.J.; Cochrane, M.A.; D’antonio, C.M.; DeFries, R.; Johnston, F.H.; Keeley, J.E.; Krawchuk, M.A.; et al. The human dimension of fire regimes on Earth: The human dimension of fire regimes on Earth. *J. Biogeogr.* **2011**, *38*, 2223–2236. [[CrossRef](#)]
53. Calkin, D.E.; Gebert, K.M.; Jones, J.G.; Neilson, R.P. Forest Service Large Fire Area Burned and Suppression Expenditure Trends, 1970–2002. *J. For.* **2005**, *103*, 179–183. [[CrossRef](#)]
54. Dunn, C.J.; DO’Connor, C.; Abrams, J.; Thompson, M.P.; Calkin, D.E.; Johnston, J.D.; Stratton, R.; Gilbertson-Day, J. Wildfire risk science facilitates adaptation of fire-prone social-ecological systems to the new fire reality. *Environ. Res. Lett.* **2020**, *15*, 025001. [[CrossRef](#)]
55. Calkin, D.E.; Cohen, J.D.; Finney, M.A.; Thompson, M.P. How risk management can prevent future wildfire disasters in the wildland-urban interface. *Proc. Natl. Acad. Sci. USA* **2014**, *111*, 746–751. [[CrossRef](#)]
56. Halofsky, J.E.; Peterson, D.L.; O’Halloran, K.A.; Hoffman, C.H. *Adapting to Climate Change at Olympic National Forest and Olympic National Park*; U.S. Department of Agriculture, Forest Service, Pacific Northwest Research Station: Portland, OR, USA, 2011.
57. Halofsky, J.E.; Peterson, D.L.; Prendeville, H.R. Assessing vulnerabilities and adapting to climate change in northwestern U.S. forests. *Clim. Chang.* **2018**, *146*, 89–102. [[CrossRef](#)]
58. Halofsky, J.S.; Conklin, D.R.; Donato, D.C.; Halofsky, J.E.; Kim, J.B. Climate change, wildfire, and vegetation shifts in a high-inertia forest landscape: Western Washington, U.S.A. *PLoS ONE* **2018**, *13*, e0209490. [[CrossRef](#)]
59. Sheehan, T.; Bachelet, D.; Ferschweiler, K. Projected major fire and vegetation changes in the Pacific Northwest of the conterminous United States under selected CMIP5 climate futures. *Ecol. Model.* **2015**, *317*, 16–29. [[CrossRef](#)]
60. Creutzburg, M.K.; Scheller, R.M.; Lucash, M.S.; LeDuc, S.D.; Johnson, M.G. Forest management scenarios in a changing climate: Trade-offs between carbon, timber, and old forest. *Ecol. Appl.* **2017**, *27*, 503–518. [[CrossRef](#)] [[PubMed](#)]
61. Parisien, M.-A.; Dawe, D.A.; Miller, C.; Stockdale, C.A.; Armitage, O.B. Applications of simulation-based burn probability modelling: A review. *Int. J. Wildland Fire* **2019**, *28*, 913–926. [[CrossRef](#)]
62. Thompson, M.P.; Gilbertson-Day, J.W.; Scott, J.H. Integrating Pixel- and Polygon-Based Approaches to Wildfire Risk Assessment: Application to a High-Value Watershed on the Pike and San Isabel National Forests, Colorado, USA. *Environ. Model. Assess.* **2016**, *21*, 1–15. [[CrossRef](#)]
63. Riley, K.L.; Loehman, R.A. Mid-21st-century climate changes increase predicted fire occurrence and fire season length, Northern Rocky Mountains, United States. *Ecosphere* **2016**, *7*, e01543. [[CrossRef](#)]
64. Scott, J.; Helmbrecht, D.; Thompson, M.P.; Calkin, D.E.; Marcille, K. Probabilistic assessment of wildfire hazard and municipal watershed exposure. *Nat. Hazards* **2012**, *64*, 707–728. [[CrossRef](#)]
65. Jurjevich, J.R.; Chun, N.; Rancik, K.; Proehl, R.; Michel, J.; Harada, M.; Rynerson, C.; Morris, R. *Coordinated Population Forecast for Clackamas County, Its Urban Growth Boundaries (UGB) and Area Outside UGB*; Population Research Center, Portland State University: Portland, OR, USA, 2017.
66. USDA Forest Service. Forest to Faucets: Forest Importance to Drinking Water Layer. 2011. Available online: <http://www.arcgis.com/home/item.html?id=5a35484eba6c428bb1a0185729e7e6ff> (accessed on 1 July 2020).

67. Weidner, E.; Todd, A. *From the Forest to the Faucet: Drinking Water and Forests in the US: Methods Paper*; USDA Forest Service Ecosystem Services & Market Program Area and State and Private Forestry: Washington, DC, USA, 2011.
68. Oregon Department of Forestry. Oregon Land Manager Layer. Oregon Spatial Data Library. 2015. Available online: <https://spatialdata.oregonexplorer.info/geoportals/details?id=9b644e0f7a7d4124a50f6b35c05626ae> (accessed on 1 July 2020).
69. Simpson, M. *Modeled Potential Vegetation Zones of Washington and Oregon*; U.S. Department of Agriculture, Forest Service, Central Oregon Area Ecology and Forest Health Program: Bend, OR, USA, 2013; Available online: <https://ecoshare.info/category/gis-datavegzones/> (accessed on 8 May 2020).
70. Haugo, R.; Zanger, C.; DeMeo, T.; Ringo, C.; Shlisky, A.; Blankenship, K.; Simpson, M.; Mellen-McLean, K.; Kertis, J.; Stern, M. A new approach to evaluate forest structure restoration needs across Oregon and Washington, USA. *For. Ecol. Manag.* **2015**, *335*, 37–50. [[CrossRef](#)]
71. Graves, D.; Chang, H. Hydrologic impacts of climate change in the Upper Clackamas River Basin, Oregon, USA. *Clim. Res.* **2007**, *33*, 143–157. [[CrossRef](#)]
72. Ingebritsen, S.E.; Sherrod, D.R.; Mariner, R.H. Rates and patterns of groundwater flow in the Cascade Range Volcanic Arc, and the effect on subsurface temperatures. *J. Geophys. Res.* **1992**, *97*, 4599. [[CrossRef](#)]
73. LANDFIRE 1.4.0. Fire Regime Class Layer 2014. Available online: <https://www.landfire.gov/fuel.php> (accessed on 1 June 2018).
74. Short, K.C. *Spatial Wildfire Occurrence Data for the United States, 1992–2015 [FPA_FOD_20170508]*, 4th ed.; Forest Service Research Data Archive: Fort Collins, CO, USA, 2017.
75. Finney, M.A.; McHugh, C.W.; Grenfell, I.C.; Riley, K.L.; Short, K.C. A simulation of probabilistic wildfire risk components for the continental United States. *Stoch. Environ. Res. Risk Assess.* **2011**, *25*, 973–1000. [[CrossRef](#)]
76. Parisien, M.A.; Ager, A.A.; Barros, A.M.; Dawe, D.; Erni, S.; Finney, M.A.; McHugh, C.W.; Miller, C.; Parks, S.A.; Riley, K.L.; et al. Commentary on the article “Burn probability simulation and subsequent wildland fire activity in Alberta, Canada—Implications for risk assessment and strategic planning” by J.L. Beverly and N. McLoughlin. *For. Ecol. Manag.* **2020**, *460*, 117698. [[CrossRef](#)]
77. Thompson, M.; Scott, J.; Langowski, P.; Gilbertson-Day, J.; Haas, J.; Bowne, E. Assessing Watershed-Wildfire Risks on National Forest System Lands in the Rocky Mountain Region of the United States. *Water* **2013**, *5*, 945–971. [[CrossRef](#)]
78. Thompson, M.P.; Scott, J.; Helmbrecht, D.; Calkin, D.E. Integrated wildfire risk assessment: Framework development and application on the Lewis and Clark National Forest in Montana, USA. *Integr. Environ. Assess. Manag.* **2013**, *9*, 329–342. [[CrossRef](#)] [[PubMed](#)]
79. Bradshaw, L.; Jolly, M. *Fire Family Plus Version 4.0*; USDA, US Forest Service Rocky Mountain Research Station: Fort Collins, CO, USA, 2008.
80. Andrews, P.L.; Loftsgaarden, D.O.; Bradshaw, L.S. Evaluation of fire danger rating indexes using logistic regression and percentile analysis. *Int. J. Wildland Fire* **2003**, *12*, 213. [[CrossRef](#)]
81. Cohen, J.D.; Deeming, J.E. *The National Fire-Danger Rating System: Basic Equations*; U.S. Department of Agriculture, Forest Service, Pacific Southwest Forest and Range Experiment Station: Berkeley, CA, USA, 1985.
82. Rupp, D.E.; Abatzoglou, J.T.; Mote, P.W. Projections of 21st century climate of the Columbia River Basin. *Clim. Dyn.* **2017**, *49*, 1783–1799. [[CrossRef](#)]
83. Abatzoglou, J.T.; Brown, T.J. A comparison of statistical downscaling methods suited for wildfire applications. *Int. J. Climatol.* **2012**, *32*, 772–780. [[CrossRef](#)]
84. LANDFIRE 1.4.0. Canopy Height Layer 2014. Available online: <https://www.landfire.gov/fuel.php> (accessed on 1 June 2018).
85. LANDFIRE 1.4.0. Canopy Base Height Layer 2014. Available online: <https://www.landfire.gov/fuel.php> (accessed on 1 June 2018).
86. LANDFIRE 1.4.0. Canopy Bulk Density Layer 2014. Available online: <https://www.landfire.gov/fuel.php> (accessed on 1 June 2018).
87. LANDFIRE 1.4.0. Canopy Cover Layer 2014. Available online: <https://www.landfire.gov/fuel.php> (accessed on 1 June 2018).
88. LANDFIRE 1.4.0. Aspect Layer 2014. Available online: <https://www.landfire.gov/topographic.php> (accessed on 1 June 2018).

89. LANDFIRE 1.4.0. Elevation Layer 2014. Available online: <https://www.landfire.gov/topographic.php> (accessed on 1 June 2018).
90. LANDFIRE 1.4.0. Slope Layer 2014. Available online: <https://www.landfire.gov/topographic.php> (accessed on 1 June 2018).
91. LANDFIRE 1.4.0. 40 Scott and Burgan Fire Behavior Fuel Models Layer 2014. Available online: <https://landfire.gov/fbfm40.php> (accessed on 1 June 2018).
92. R Core Team. *R: A Language and Environment for Statistical Computing*; R Foundation for Statistical Computing: Vienna, Austria, 2018.
93. Riley, K.L.; Abatzoglou, J.T.; Grenfell, I.C.; Klene, A.E.; Heinsch, F.A. The relationship of large fire occurrence with drought and fire danger indices in the western USA, 1984–2008: The role of temporal scale. *Int. J. Wildland Fire* **2013**, *22*, 894. [[CrossRef](#)]
94. Riley, K.; Thompson, M.; Scott, J.; Gilbertson-Day, J. A Model-Based Framework to Evaluate Alternative Wildfire Suppression Strategies. *Resources* **2018**, *7*, 4. [[CrossRef](#)]
95. Cumming, S.G. A parametric model of the fire-size distribution. *Can. J. For. Res.* **2001**, *31*, 1297. [[CrossRef](#)]
96. Moritz, M.A. Analyzing Extreme Disturbance Events: Fire in Los Padres National Forest. *Ecol. Appl.* **1997**, *7*, 1252–1262. [[CrossRef](#)]
97. Jiang, Y.; Zhuang, Q. Extreme value analysis of wildfires in Canadian boreal forest ecosystems. *Can. J. For. Res.* **2011**, *41*, 1836–1851. [[CrossRef](#)]
98. Gilleland, E. extRemes: Functions for Performing Extreme Value Analysis. R Package Version 2.01-2. 2020. Available online: <https://cran.r-project.org/web/packages/extRemes/extRemes.pdf> (accessed on 1 July 2020).
99. Moody, J.A.; Martin, D.A.; Haire, S.L.; Kinner, D.A. Linking runoff response to burn severity after a wildfire. *Hydrol. Process.* **2008**, *22*, 2063–2074. [[CrossRef](#)]
100. Emelko, M.B.; Silins, U.; Bladon, K.D.; Stone, M. Implications of land disturbance on drinking water treatability in a changing climate: Demonstrating the need for “source water supply and protection” strategies. *Water Res.* **2011**, *45*, 461–472. [[CrossRef](#)] [[PubMed](#)]
101. Halleme, D.W.; Sun, G.; Caldwell, P.V.; Norman, S.P.; Cohen, E.C.; Liu, Y.; Bladon, K.D.; McNulty, S.G. Burned forests impact water supplies. *Nat. Commun.* **2018**, *9*, 1307. [[CrossRef](#)] [[PubMed](#)]
102. Schwalm, C.R.; Glendon, S.; Duffy, P.B. RCP8.5 tracks cumulative CO₂ emissions. *Proc. Natl. Acad. Sci. USA* **2020**, *117*, 19656–19657. [[CrossRef](#)] [[PubMed](#)]
103. Hausfather, Z.; Peters, G.P. RCP8.5 is a problematic scenario for near-term emissions. *Proc. Natl. Acad. Sci. USA* **2020**, *117*, 27791–27792. [[CrossRef](#)] [[PubMed](#)]
104. Gilbertson-Day, J.; Stratton, R.D.; Scott, J.H.; Vogler, K.C.; Brough, A. Pacific Northwest Quantitative Wildfire Risk Assessment: Methods and Results. 2018. Available online: <http://pyrologix.com/wp-content/uploads/2019/11/PNW%20Quantitative%20Wildfire%20Risk%20Assessment%20Report%204-9-2018%20v2.pdf> (accessed on 1 July 2020).
105. Millar, C.I.; Stephenson, N.L. Temperate forest helath in the era of emerging megadisasters. *Science* **2015**, *349*, 823–826. [[CrossRef](#)] [[PubMed](#)]
106. Tepley, A.J.; Thomann, E.; Veblen, T.T.; Perry, G.L.; Holz, A.; Paritsis, J.; Kitzberger, T.; Anderson-Teixeira, K.J. Influences of fire-vegetation feedbacks and post-fire recovery rates on forest landscape vulnerability to altered fire regimes. *J. Ecol.* **2018**, *106*, 1925–1940. [[CrossRef](#)]
107. Byram, G.M. Combustion of forest fuels. *For. Fire Control Use* **1959**, 61–89.
108. Scott, J.H. Introduction to Wildfire Behavior Modeling. National Interagency Fuels, Fire & Vegetation Technology Transfer. 2012. Available online: www.nift.gov (accessed on 10 December 2018).
109. Nelson, K.N.; Turner, M.G.; Romme, W.H.; Tinker, D.B. Simulated fire behaviour in young, postfire lodgepole pine forests. *Int. J. Wildland Fire* **2017**, *26*, 852. [[CrossRef](#)]
110. Wotton, B.M.; Flannigan, M.D.; Marshall, G.A. Potential climate change impacts on fire intensity and key wildfire suppression thresholds in Canada. *Environ. Res. Lett.* **2017**, *12*, 095003. [[CrossRef](#)]
111. Lozano, O.M.; Salis, M.; Ager, A.A.; Arca, B.; Alcasena, F.J.; Monteiro, A.T.; Finney, M.A.; Del Giudice, L.; Scoccimarro, E.; Spano, D. Assessing Climate Change Impacts on Wildfire Exposure in Mediterranean Areas: Climate Change Impacts on Mediterranean Wildfires. *Risk Anal.* **2017**, *37*, 1898–1916. [[CrossRef](#)] [[PubMed](#)]
112. Keeley, J.E. Fire intensity, fire severity and burn severity: A brief review and suggested usage. *Int. J. Wildland Fire* **2009**, *18*, 116. [[CrossRef](#)]

113. Hirsch, K.; Martell, D. A Review of Initial Attack Fire Crew Productivity and Effectiveness. *Int. J. Wildland Fire* **1996**, *6*, 199. [[CrossRef](#)]
114. Cruz, M.G.; Alexander, M.E. Assessing crown fire potential in coniferous forests of western North America: A critique of current approaches and recent simulation studies. *Int. J. Wildland Fire* **2010**, *19*, 377. [[CrossRef](#)]
115. Stavros, E.N.; Abatzoglou, J.T.; McKenzie, D.; Larkin, N.K. Regional projections of the likelihood of very large wildland fires under a changing climate in the contiguous Western United States. *Clim. Chang.* **2014**, *126*, 455–468. [[CrossRef](#)]
116. Wang, X.; Studens, K.; Parisien, M.A.; Taylor, S.W.; Candau, J.N.; Boulanger, Y.; Flannigan, M.D. Projected changes in fire size from daily spread potential in Canada over the 21st century. *Environ. Res. Lett.* **2020**, *15*, 104048. [[CrossRef](#)]
117. Millar, C.I.; Stephenson, N.L.; Stephens, S.L. Climate Change and Forests of the Future: Managing in the Face of Uncertainty. *Ecol. Appl.* **2007**, *17*, 2145–2151. [[CrossRef](#)]
118. Schoennagel, T.; Balch, J.K.; Brenkert-Smith, H.; Dennison, P.E.; Harvey, B.J.; Krawchuk, M.A.; Mietkiewicz, N.; Morgan, P.; Moritz, M.A.; Rasker, R.; et al. Adapt to more wildfire in western North American forests as climate changes. *Proc. Natl. Acad. Sci. USA* **2017**, *114*, 4582–4590. [[CrossRef](#)]
119. Podur, J.; Wotton, M. Will climate change overwhelm fire management capacity? *Ecol. Model.* **2010**, *221*, 1301–1309. [[CrossRef](#)]
120. Gebert, K.M.; Calkin, D.E.; Yoder, J. Estimating Suppression Expenditures for Individual Large Wildland Fires. *West. J. Appl. For.* **2007**, *22*, 188–196. [[CrossRef](#)]
121. Barros, A.M.; Ager, A.A.; Day, M.A.; Palaiologou, P. Improving long-term fuel treatment effectiveness in the National Forest System through quantitative prioritization. *For. Ecol. Manag.* **2019**, *433*, 514–527. [[CrossRef](#)]
122. Barnett, K.; Miller, C.; Venn, T.J. Using Risk Analysis to Reveal Opportunities for the Management of Unplanned Ignitions in Wilderness. *J. For.* **2016**, *114*, 610–618. [[CrossRef](#)]
123. Thompson, M.P.; Bowden, P.; Brough, A.; Scott, J.H.; Gilbertson-Day, J.; Taylor, A.; Anderson, J.; Haas, J.R. Application of Wildfire Risk Assessment Results to Wildfire Response Planning in the Southern Sierra Nevada, California, USA. *Forests* **2016**, *7*, 64. [[CrossRef](#)]

Publisher’s Note: MDPI stays neutral with regard to jurisdictional claims in published maps and institutional affiliations.



© 2020 by the authors. Licensee MDPI, Basel, Switzerland. This article is an open access article distributed under the terms and conditions of the Creative Commons Attribution (CC BY) license (<http://creativecommons.org/licenses/by/4.0/>).